

# Intraoceanic subduction of “heterogeneous” oceanic lithosphere in narrow basins: 2D numerical modeling

Cristina Malatesta <sup>a,\*</sup>, Taras Gerya <sup>b</sup>, Marco Scambelluri <sup>a</sup>, Laura Federico <sup>a</sup>,  
Laura Crispini <sup>a</sup>, Giovanni Capponi <sup>a</sup>

<sup>a</sup> Dipartimento per lo Studio del Territorio e delle sue Risorse, Università di Genova, corso Europa 26, 16132 Genova Italy

<sup>b</sup> Institute of Geophysics, ETH Zentrum, Sonneggstrasse 5, 8092 Zürich Switzerland

## ARTICLE INFO

### Article history:

Received 16 June 2011

Accepted 5 January 2012

Available online 13 January 2012

### Keywords:

Intraoceanic subduction

Numerical modeling

HP-rocks exhumation

Narrow oceanic basin

Serpentinite channel

## ABSTRACT

We provide 2D thermomechanical numerical models to constrain the subduction process of narrow (~ 600 km wide) oceanic basins resulting in formation and exhumation of serpentinite-bearing high-pressure (HP) and ultrahigh-pressure (UHP) complexes presently exposed as dismembered massifs in orogenic belts. We simulated subduction of “heterogeneous” (i.e. non layered) oceanic lithosphere testing different serpentinite rheologies and varying other major parameters (initial slab dip, convergence rate, age and structure of oceanic lithosphere, distance subduction zone/continental margin, weak zone geometry). We show that serpentinite rheology is the most important parameter affecting both the geometry and behavior of serpentinite channels that form in the mantle-wedge as the result of upward migration of slab fluids. A strong serpentinite power-law rheology is responsible for the continuous accretion and underthrusting of slab slices at the base of mantle-wedge to form planar- or wedge-shape serpentinitic channels; the great part of sediments is buried only during continental crust subduction but is never exhumed; moreover slab slices do not mix with mantle wedge rocks. Exhumation of mafic/ultramafic rocks occurs from pressure not exceeding 15 kbar. On the other hand, a weak Newtonian behavior of serpentine best describes subduction and exhumation dynamics. This rheology produces channels that usually widen to depth; slab and sediment slices are easily incorporated in mantle wedge serpentinite during ongoing convergence; in this case, slab and mantle-wedge serpentinite are mixed together and can be closely associated in the channel. The models running a Newtonian rheology highlight that slices of the oceanic overriding plate can be eroded and dragged in the channel till great depth. A weak power-law serpentinite rheology produces a transitional behavior between that of strong power-law and Newtonian rheology. The serpentinitic mélange, produced using a Newtonian rheology, is finally exhumed from pressure >20 kbar during the final stages of continental crust subduction and collision. The rise to shallow depth of the HP mélange is driven by concurrent serpentinite buoyancy, slab roll-back and asthenospheric mantle upwelling. Moreover, we propose that the subduction/exhumation dynamics observed in the model acted during closure of the narrow Alpine Tethys ocean; in particular, we suggest that some slices presently outcropping in HP ophiolitic massifs of the Western Alps (Voltri and Monviso massifs) were tectonically coupled at slab/mantle interface and exhumed during collision in a soft, low-viscosity serpentinite channel.

We finally investigated intensity and dynamics of magmatic processes during subduction. Our numerical experiments suggest that even subduction of narrow oceanic basins may indeed allow the development of a magmatic arc. In such relatively small short-living arcs, steeper, faster and younger slabs produce earlier onset of the volcanism after the beginning of subduction.

© 2012 Elsevier B.V. All rights reserved.

## 1. Introduction

Several high-pressure (HP) and ultra high-pressure (UHP) terrains in the world are related to subduction and closure of narrow (i.e. up to 1300 km-wide) inter-continental oceanic basins (e.g. Alps, Zagros,

Sistan; Agard et al., 2009; Marroni and Pandolfi, 2007; McQuarrie et al., 2003). More specifically, *intraoceanic* subduction is responsible for the closure of some of these basins. In addition, intra-oceanic plate margins constitute about 40% of the present-day subduction zones on Earth (Leat and Larter, 2003).

Tectonic uprise and emplacement of eclogite-facies rocks in mountain buildings has been explained through a number of major processes, included exhumation along the slab/mantle interface. Starting from the subduction-channel model by Cloos (1982)

\* Corresponding author.

E-mail address: [cristina.malatesta@unige.it](mailto:cristina.malatesta@unige.it) (C. Malatesta).

conceived to explain exhumation of high pressure blocks in a sedimentary matrix, an increasing number of studies has envisaged that exhumation is localized in a low-viscosity weak zone at the plate interface where upward flow of high- and ultrahigh-pressure slices accreted to this channel is strongly enhanced. The large stability field of antigorite serpentinite to maximum depths of about 200 km (Ulmer and Trommsdorff, 1995), provides reliable evidence for serpentinization of the mantle wedge flushed by subduction fluids (Bostock et al., 2002; Hyndman and Peacock, 2003) and for the presence of weak serpentinite layers atop of the slab. Several models and natural occurrences now suggest that exhumation of HP rocks involved in intraoceanic subduction likely occurs inside serpentinite channels (i.e. Agard et al., 2009; Blanco-Quintero et al., 2011a; Gerya et al., 2002; Gorczyk et al., 2007; Guillot et al., 2009; Krebs et al., 2011). High-pressure low-temperature rocks exhumed along serpentinite channels correspond to cm to km-sized weakly deformed lenses of former oceanic-crustal rocks surrounded by prevalent highly sheared serpentinites. Metasediments are generally subordinate in volume and are highly deformed (e.g. Rio San Juan Complex in Dominican Republic, Krebs et al., 2011 and references therein; Sierra del Convento and La Corea serpentinite matrix mélanges, eastern Cuba, Blanco-Quintero et al., 2011a; García-Casco et al., 2006; Monviso Massif in Western Alps, Guillot et al., 2009; Schwartz et al., 2000; Schwartz et al., 2007; Voltri Massif in Western Alps, Federico et al., 2007; Malatesta et al., 2011). Numerical models of subduction have been provided for general case-studies involving burial of oceanic plates below continental margins, or intraoceanic subduction within infinitely large basins (e.g. Arcay et al., 2005; Burov et al., 2001; Faccenda et al., 2009; Gerya and Stöckhert, 2006; Gerya et al., 2002; Gorczyk et al., 2007; Meda et al., 2010; Roda et al., 2010; Schwartz et al., 2001; Warren et al., 2008; Yamato et al., 2007, 2008, 2009). These models apply to geodynamic settings like Japan, Andes and to orogenic terrains like those domains of the Alps where oceanic subduction was below a thinned continental margin. Still untested is the process of intraoceanic subduction within a narrow basin. This could shed light on subsystems of the Alpine orogen like Western Liguria, where subduction was intraoceanic (Abbate et al., 1980; Boccaletti et al., 1971; Hoogerduijn Strating, 1991; Marroni and Treves, 1998; Marroni et al., 2010 and references therein; Van Wamel, 1987).

In our models, the inferred width of the oceanic basin is comparable to the extension of past oceanic basins, ranging from <600 km (e.g. Western Tethys; Marroni and Pandolfi, 2007) to 1300 km (e.g. Neotethys) (McQuarrie et al., 2003). These fossil basins were characterized either by layered (complete) oceanic lithosphere (Neotethys; Dilek et al., 1991) or by “incomplete” oceanic sequences (Western Tethys; Lagabriele and Cannat, 1990; Lagabriele and Lemoine, 1997; Piccardo, 2007). In the layered oceanic lithosphere, like in fast spreading centers, mantle peridotites are overlain by layered gabbros that grade towards a sheeted dyke complex covered by massive and pillow basalts at the top. The incomplete sequences, like the present-day slow or ultra-slow spreading ridges (with spreading rate of about 55 mm/y and <12 mm/y, respectively; Dick et al., 2003), are characterized by magma starved segments where gabbros form limited bodies inside the oceanic mantle and the sheeted dike complex is lacking. In the latter settings serpentinitized mantle peridotites occupy large areas of the ocean floor (Mevel, 2003).

Numerical modeling of subduction of heterogeneous crust produced at slow spreading ridges is scarce. Single numerical study of Gorczyk et al. (2007) focused on the Caribbean setting, tested intraoceanic subduction in which the upper plate is a classical oceanic crust and the lower plate is a “low-spreading oceanic crust”. They noticed that subduction of such oceanic lithosphere, at a convergence rate of 2 cm/y, produces a wide subduction channel made of serpentinites (hydrated abyssal peridotite and hydrated mantle peridotite), metabasalts, metagabbros and minor metasediments. Gorczyk et al.

(2007) also concluded that serpentinite buoyancy is the driving force that allows the rise of serpentinite mélanges through extension zones induced by the slab retreat. Indeed, the results of this study cannot be directly applied to the Western Alpine Tethys where the extent of oceanic subduction was much shorter than in the Caribbean and culminated by subduction of passive margin.

The aim of this paper is to present a new 2D model of intraoceanic subduction of “heterogeneous” oceanic lithosphere in narrow basins that culminates with passive margin subduction and to compare numerical results with the natural case of the Western Alpine Tethys.

Moreover, we test how geometric (initial dip angle of the slab, distance of the subduction zone from continental margins, extent of serpentinization in abyssal peridotite, weak zone geometry), kinematic (convergence rate) and rheological parameters (rheology of serpentinite, age of oceanic lithosphere) can affect evolution of this intraoceanic subduction. We performed 2D numerical simulations using the modified code I2VIS (Gerya and Yuen, 2003, 2007). The coupled petrological–thermomechanical models allow a self-organization of the subduction zone geometry that is free to evolve spontaneously. In particular we analyzed the potential development of a serpentinite channel localized at the slab/mantle interface and the exhumation trajectories of high-pressure rocks inside the channel. We also investigated possible magmatic activity and crust formation produced by partial melting above the slab in order to find out if subduction of a narrow oceanic basin is able to produce a magmatic arc.

## 2. Model description

The subduction model adopted here is similar to previous numerical studies (Gorczyk et al., 2007; Sizova et al., 2010). It is designed in a 4000 km × 200 km box in which computational finite-difference nodes are distributed on an irregular rectangular 2001 × 2001 grid (resolution changes from 1 × 1 km in the central area to 5 × 1 km on the margins of the model); 13 million markers are randomly distributed inside the grid. All mechanical boundary conditions are free-slip with the exception of the lower boundary that is permeable.

We reproduced behavior of a relatively narrow, about 600 km wide, oceanic basin delimited by thinned continental margins (Fig. 1). The lithosphere in this basin is significantly different from the layered lithosphere typical of fast spreading ridges, as it dominantly consists of variably serpentinitized peridotites hosting km-size intrusive gabbroic bodies capped by a thin discontinuous basaltic layer. Such “heterogeneous” lithosphere is often related to slow and ultra-slow spreading ridges (Dick et al., 2003, 2006; Ildefonse et al., 2007; Lagabriele and Lemoine, 1997; Mevel, 2003; Piccardo, 2007). In our models the gabbroic bodies have fixed sizes (1 × 1 km or 2 × 2 km) and are arranged in rows with horizontal spacing respectively of 1 and 2 km (Fig. 1). The vertical distance of the rows is 1 km. The size and the spacing of the bodies are comparable to the grid size that precludes accurate modeling of shapes and internal deformation of individual bodies. Indeed, due to the high density of Lagrangian markers and the use of local marker-to-node interpolation schemes (Duretz et al., 2011; Gerya and Yuen, 2007), disintegration and mechanical mixing of the heterogeneous oceanic crust in subduction channel is resolved in the models that is sufficient for the purpose of our study.

The discontinuous basaltic layer is arranged in blocks (500 m thick, 2 km wide), separated by 2 km of serpentinite representing topographic highs in the basin. Both are overlain by a 1 km-thick sedimentary cover.

The continental margins in the models are characterized by a wet quartzite rheology (Ranalli, 1995). The continental crust has maximum thickness of 30 km and becomes thinner near the contact with the serpentinitized oceanic lithosphere. A sedimentary cover is present also on continental margins.

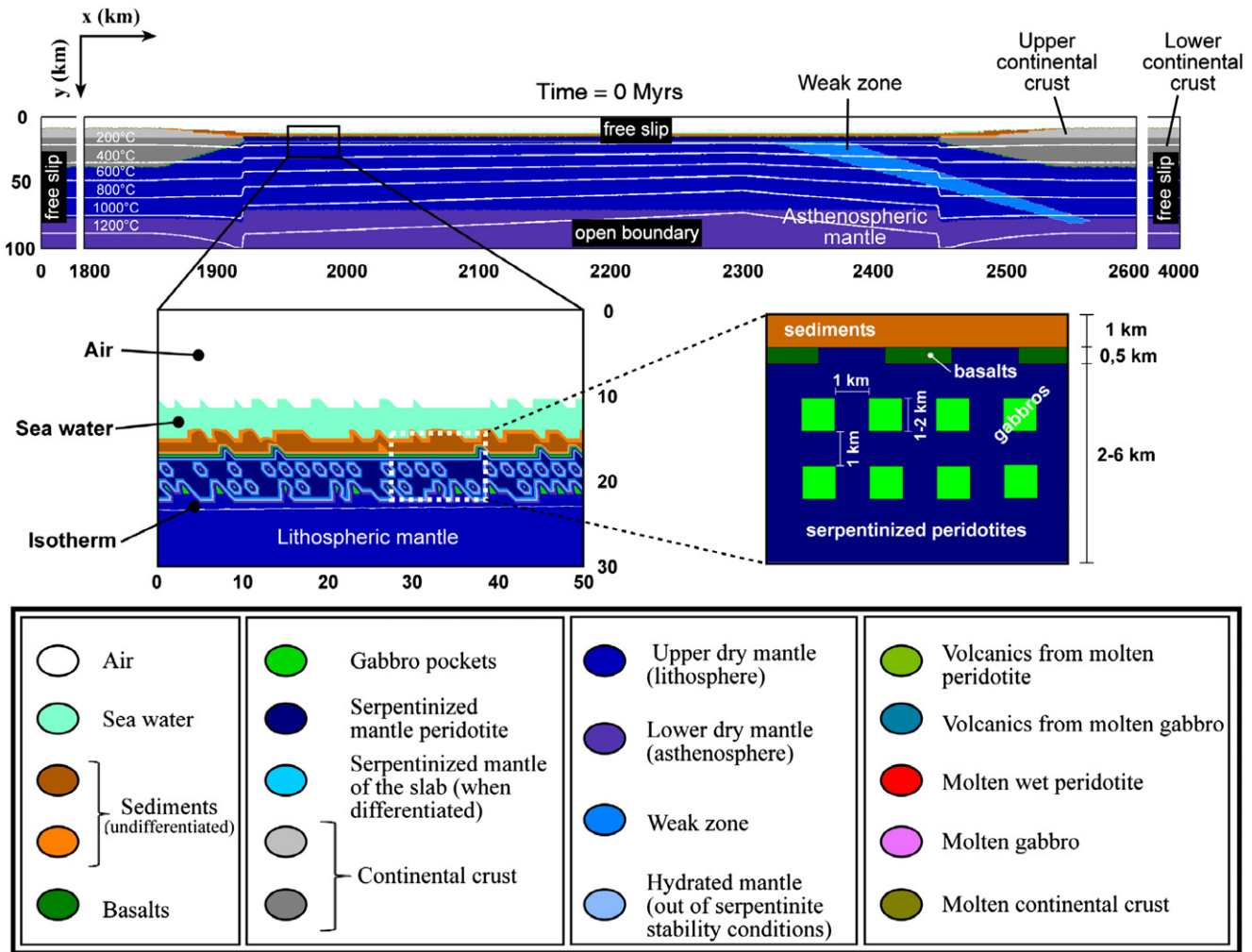


**Fig. 1.** Initial set up of the models. An oceanic basin delimited by continental margins is depicted. The oceanic lithosphere structure is peculiar of slow and ultra-slow spreading ridges: gabbros are present as pockets inside the serpentinized lithospheric mantle; a discontinuous basaltic layer covers the serpentinized peridotites which form topographic highs in the basin. Sediments overlie both the oceanic lithosphere and the distal part of the continental margins. The size of gabbro intrusions and the thickness of the serpentinite horizon can vary in the models as described in Table 2.

The upper layer of the model (from 8 km to 13 km above the continental crust and the oceanic lithosphere, respectively) consists of low-density and low-viscosity media corresponding respectively to air (density =  $1 \text{ kg/m}^3$ , viscosity =  $10^{19} \text{ Pa s}$ ) and sea water (density =  $1000 \text{ kg/m}^3$ , viscosity =  $10^{19} \text{ Pa s}$ ). The high viscosity contrast between such media and the oceanic or continental lithosphere minimizes shear stresses ( $< 10^5 \text{ Pa}$ ) at the top of the solid portion of the model, that behaves as a free erosion/sedimentation surface (Nikolaeva et al., 2008; Schmeling et al., 2008).

Horizontal plate motion is simulated applying a prescribed constant velocity (Table 2a–b) to a narrow area placed in the “left-side” continental lithosphere.

Erosion and sedimentation are controlled by a transport equation (Nikolaeva et al., 2008) which comprises imposed erosion ( $v_e = 0.3 \text{ mm/y}$ ) and sedimentation rates ( $v_s = 0.03 \text{ mm/y}$ ), as well as erosion and sedimentation levels. The depth under which sedimentation begins coincides with sea level. The surface slope for the accumulated sedimentary prism is limited by  $27^\circ$ . The density and viscosity of rocks are calculated for given P–T conditions (Table 1).

An oceanic geotherm (Turcotte and Schubert, 2002) defines the initial temperature field of the oceanic plates. The thermal structure of the oceanic lithosphere simulates an asymmetrical opening of the basin (Fig. 1); the age decreases from the transitional zones (55 My), close to the continental margins, towards the inner area of

the basin (Table 2). A particular geotherm characterizes the temperature field of the transitional zones between the ocean and the continental margins.

After bending of the oceanic lithosphere, subduction starts at a geometrically prescribed weak zone that represents the decoupling area between the two plates. It virtually corresponds to a shear zone that dips in the mantle and that is characterized by a wet olivine rheology (Ranalli, 1995). We considered a “right”-dipping weak zone 60 km-thick at the top, 20 km-thick at the bottom and reaching 80 km depth. In our models the dip angle of the weak zone controls the initial inclination of the subducting slab.

At the beginning of subduction, sediments are scraped off the downgoing plate and are piled up in the accretionary wedge that progressively forms during convergence.

During convergence, the subducted lithosphere and the hydrated overlying mantle gradually replace the weak zone, thus maintaining decoupling along the plate interface. In order to analyze the influence of the weak zone geometry on subduction models, we also conducted few runs with a trapezium-shape weak zone (230 km-thick at the top, 20 km-thick at the bottom and 40 km deep) with friction coefficients varying from 0.1 to 0.3.

As soon as subduction starts along the weak zone, the entire system and the dip angle of the slab are free to evolve. The inclination of the subducting plate during the process is mainly affected by its

**Table 1**  
Physical properties of rocks used in numerical simulations.  $\rho_0$  = density;  $k$  = thermal conductivity;  $T_{\text{solidus,liquidus}}$  = solidus and liquidus temperatures of the crust;  $H_r$ ,  $H_L$  = heat production (radiogenic, latent);  $E$  = activation energy;  $n$  = stress component;  $A_D$  = material constant,  $V$  = activation volume;  $\sin(\varphi_{\text{dry}})$  = effective friction coefficient for dry rocks. The following parameters are the same for all the rocks:  $C_p = 1000 \text{ J/kg}$ ,  $a = 3 \times 10^{-5} \text{ K}^{-1}$ ,  $b = 1 \times 10^{-3} \text{ MPa}^{-1}$ .

Material	$\rho_0$ , [kg/m <sup>3</sup> ]	$k$ [W/(m·K)]	$T_{\text{solidus}}$ [K]	$T_{\text{liquidus}}$ [K]	$H_r$ [ $\mu\text{W/m}^3$ ]	$H_L$ [kJ/kg]	$E$ [kJ/mol]	$n$	$A_D$ [ $\text{MPa}^{-n} \cdot \text{s}^{-1}$ ]	$V$ [J/ ( $\text{MPa} \cdot \text{mol}$ )]	Rheology/flow law
Sediments and felsic crust	Sediments: 2600 Felsic crust: 2700	$[0.64 + 807 / (T + 77)] \times \exp(0.00004 \cdot P_{\text{MPa}})$	At $P < 1 \text{ MPa}$ : $889 + 17,900 / (P + 54) + 20,200 / (P + 54)^2$ . At $P > 1200 \text{ MPa}$ : $831 + 0.06 \cdot P$	$1262 + 0.009 \cdot P$	Sed.:2 Felsic crust:1	300	154	2.3	$10^{-3.5}$	0	Wet quartzite, $c = 10 \text{ MPa}$ , $\sin(\varphi_{\text{dry}}) = 0.15$
Melt-bearing sediments and felsic crust	2400	–	–	–	–	–	0	1	–	–	
Basalts	3000	$[1.18 + 474 / (T + 77)] \times \exp(0.00004 \cdot P_{\text{MPa}})$	At $P < 1600 \text{ MPa}$ : $973 - 70,400 / (P + 354) + 77,800,000 / (P + 354)^2$ . At $P > 1600 \text{ MPa}$ : $935 + 0.0035 \cdot P + 0.0000062 \cdot P^2$	$1423 + 0.105 \cdot P$	0.25	380	154	2.3	$10^{-3.5}$	0	Wet quartzite, $c = 10 \text{ MPa}$ , $\sin(\varphi_{\text{dry}}) = 0.1$
Melt-bearing basalts	2900	–	–	–	–	–	0	1	–	–	
Gabbroic/Mafic crust	3000	$[1.18 + 474 / (T + 77)] \times \exp(0.00004 \cdot P_{\text{MPa}})$	–	$1423 + 0.105 \cdot P$	0.25	380	238	3.2	$10^{-3.5}$	0	Plagioclase $\text{An}_{75}$ , $c = 10 \text{ MPa}$ , $\sin(\varphi_{\text{dry}}) = 0.6$
Lithosphere–Asthenosphere dry mantle	3300	$[0.73 + 1293 / (T + 77)] \times \exp(0.00004 \cdot P_{\text{MPa}})$	$1394 + 0.133 \cdot P - 0.0000051 \cdot P^2$	$2073 + 0.114 \cdot P$	0.022	–	532	3.5	$10^{4.4}$	8	Dry olivine, $c = 10 \text{ MPa}$ , $\sin(\varphi_{\text{dry}}) = 0.6$
Hydrated mantle/Hydrated mantle at subduction zone (weak zone)/Serpentinized mantle	3200 (hydrated) 3300 (weak zone) 3000 (serp.)	–	Hydrated mantle: at $P < 1600 \text{ MPa}$ : $973 + 70,400 / (P + 354) + 77,800,000 / (P + 354)^2$ . At $P > 1600 \text{ MPa}$ : $935 + 0.0035 \cdot P + 0.0000062 \cdot P^2$	Hydrated mantle: $2073 + 0.114 \cdot P$	0.022	Hydrated mantle: 300	470 $8,9^a$	4 $3,8^a$	$10^{3.3}$ $10^{-37a}$	– $3,2^a$	Wet olivine, $c = 10 \text{ MPa}$ , $\sin(\varphi_{\text{dry}}) = 0.1$ ; for Newtonian rheology: $\eta_{\text{creep}} = 10^{18} \text{ P s}$
Melt-bearing dry mantle	2900	–	–	–	–	–	0	1	–	–	
References <sup>b</sup>	1,2	3	4	5	5	1	1,2,6	4,6	4	4,6	4,1

<sup>a</sup> Weak serpentinite power-law rheology.

<sup>b</sup> 1 = (Turcotte and Schubert, 2002), 2 = (Bittner and Schmeling, 1995), 3 = (Clauser and Huenges, 1995), 4 = (Ranalli, 1995), 5 = (Schmidt and Poli, 1998), 6 = (Hilaret et al., 2007).

**Table 2**

Description of models parameters and summary of volcanic activity main features; the friction coefficient of the weak zone is zero, except for *craq* model (0.1); serpentinite in all the models have density =  $3.0 \cdot 10^3 \text{ kg/m}^3$  (50% of serpentinitization), except for *crca* (\*) model (serpentinite density =  $2.8 \cdot 10^3 \text{ kg/m}^3$ ; almost a pure serpentinite); gabbro size is  $1 \times 1 \text{ km}$ ; the distance of the weak zone from the “right” continental margin is 100 km. *Craz* and *crba* models have  $2 \times 2 \text{ km}$  gabbro size and the distance of the weak zone from the “right” margin is 150 km. \*\* Models with a layered oceanic crust. a) a strong power-law rheology of serpentinite (wet olivine) is used except for model *crdk* (weak power-law rheology, *Hilairret et al., 2007*). ( $OL_{\text{age}}$  = age of the youngest oceanic lithosphere;  $H$  = thickness of the serpentinite horizon in the slab;  $t_{\text{volc}}$  = time elapsed between subduction beginning and appearing of volcanic activity on surface;  $D_{\text{tr}}$  = distance of the first spreading site from the trench;  $E_{\text{volc}}$  = linear extension of the volcanics on surface measured after 40 My for convergence rate = 1 cm/y, 20 My for 2 cm/y and 13 My for 3 cm/y). b) Models running a weak serpentinite Newtonian rheology.

Model	Convergence rate	Slab dip	$OL_{\text{age}}$	$H$	Serp. channel geometry	Volcanic activity		
						$t_{\text{volc}}$	$D_{\text{tr}}$	$E_{\text{volc}}$
a)								
<i>crbc</i>	1 cm/y	15°	<b>30 My</b>	4 km	Planar	29 My	280 km	20 km
<i>crbe</i>	1 cm/y	15°	<b>5 My</b>	4 km	Wedge	25 My	250 km	<10 km
<i>crbl</i>	<b>3 cm/y</b>	20°	25 My	4 km	Wedge	7 My	240 km	100 km
<i>crcb</i>	<b>1 cm/y</b>	20°	25 My	4 km	Wedge/Planar	21 My	200 km	80 km (spaced spots)
<i>crbo</i>	1 cm/y	15°	25 My	4 km	Planar	30 My	270 km	<50 km (very spaced spots)
<i>crch</i>	1 cm/y	<b>40°</b>	25 My	4 km	Wedge	10 My	120 km	70 km
<i>craz</i>	1 cm/y	15°	25 My	<b>6 km</b>	Wedge	29 My	260–290 km	Spots activity
<i>crba</i>	1 cm/y	15°	25 My	<b>2 km</b>	Planar	25 My	260–280 km	25 km
<i>craq</i>	1 cm/y	–	10 My	6 km	–	–	–	–
<i>crdk</i>	1 cm/y	15°	25 My	4 km	Wedge/Planar	30 My	260 km	50 km
<i>crca</i> *	1 cm/y	15°	25 My	4 km	Planar	29 My	280 km	20 km
<i>crc*</i> **	1 cm/y	15°	25 My	–	–	26 My	260 km	70 km
b)								
<i>crck</i>	1 cm/y	<b>15°</b>	25 My	4 km	Hourglass	23 My	175 km	20 km
<i>crco</i>	1 cm/y	<b>40°</b>	25 My	4 km	Planar	10 My	110 km	40 km
<i>crcp</i>	<b>3 cm/y</b>	15°	25 My	4 km	Planar	8 My	230–240 km	40–50 km
<i>crcr</i>	1 cm/y	<b>15°</b>	<b>5 My</b>	4 km	Hourglass	24 My	210–220 km	40 km
<i>crcs</i>	1 cm/y	<b>15°</b>	<b>30 My</b>	4 km	Planar + bulge	23 My	175 km	Spots
<i>crdl</i> **	1 cm/y	15°	25 My	–	Planar	23 My	200 km	100 km

rheology and density and by the thermomechanical interaction with the surrounding material (*Gorczyk et al., 2007*).

Fluids released by the subducting slab hydrate the overlying mantle wedge (*Gerya et al., 2002; Gorczyk et al., 2007; Poli and Schmidt, 1995; Schmidt and Poli, 1998*). Fluids are subducted inside rock porosities or are fixed in hydrous minerals whose stability controls the episodes of fluid release, which can occur to depths exceeding 200 km (*Poli and Schmidt, 1995; Schmidt and Poli, 1998*). The amount of water (up to 2 wt.%) released from rock porosity (sediments and basaltic crust) is computed as a linear function of depth as follows:

$$X_{\text{H}_2\text{O}(\text{wt.}\%)} = X_{\text{H}_2\text{O}(\text{p}0)} \times (1 - \Delta z / 75)$$

where  $X_{\text{H}_2\text{O}(\text{p}0)} = 2 \text{ wt.}\%$  is the porosity water content at the surface;  $\Delta z$  is the depth below the surface in km (*Sizova et al., 2010*).

Slab mantle dehydration/hydration algorithm is based on water markers and is similar to previously published subduction models (*Gorczyk et al., 2007; Nikolaeva et al., 2008; Sizova et al., 2010*). The physicochemical conditions in the model and assumption of thermodynamic equilibrium control the dehydration reactions that allow  $\text{H}_2\text{O}$  release by a rock marker. The generated water marker includes a particular amount of water and starts to move independently with time until it reaches a lithology that can assimilate  $\text{H}_2\text{O}$  (*Sizova et al., 2010*). The velocity of fluid markers is calculated from the local kinematical transport condition as follows (*Gorczyk et al., 2007*):

$$V_{\text{x}(\text{water})} = V_{\text{x}}, V_{\text{z}(\text{water})} = V_{\text{z}} - V_{\text{z}(\text{percolation})}$$

where  $v_{\text{x}}$  and  $v_{\text{z}}$  are the local velocity of the mantle and  $v_{\text{z}(\text{percolation})}$  is the prescribed relative velocity of upward percolation of  $\text{H}_2\text{O}$  through the mantle. The maximum water content of the mantle wedge hydrated by the slab fluids is 2 wt.%. (*Sizova et al., 2010*). The boundary between serpentinite-rich and hydrated serpentinite-free mantle rocks (density =  $3200 \text{ kg/m}^3$ ) is defined by the stability field of antigorite (*Schmidt and Poli, 1998*). Furthermore we assumed that the

serpentinitization degree of mantle peridotites is described by the rock density, that in our models varies between 2800 (almost a fully serpentinitized peridotite) and  $3000 \text{ kg/m}^3$  (50% of serpentinitization; *Hilairret and Reynard, 2009*).

It is well understood that serpentinitization of mantle rocks causes their significant rheological weakening in both brittle and ductile regime of deformation (*Escartin et al., 2001; Hilairret et al., 2007; Hirose et al., 2006; Katayama et al., 2009; Tatakahashi et al., 2011*). The actual amount of weakening depends on many physical factors including degree of serpentinitization (e.g., *Escartin et al., 2001*), mineral composition, water content, ongoing hydration/dehydration reactions (e.g., *Hirose et al., 2006*), and deformation regime (e.g., *Escartin et al., 2001; Hilairret et al., 2007; Hirose et al., 2006*). Since for the natural subduction process these factors remain largely uncertain, we tested a range of different rheologies for serpentinitized mantle in our models: strong power law rheology of wet olivine (*Ranalli, 1995*), weak power law rheology of antigorite (*Hilairret et al., 2007*) and weak Newtonian rheology with the constant viscosity of  $10^{18} \text{ Pa s}$  (*Gerya et al., 2002*) (see *Table 1* for parameters of different models).

Melt is extracted from partially molten rocks considering a melt extraction threshold  $M_{\text{max}}$  and a non-extractable amount of melt  $M_{\text{min}} < M_{\text{max}}$  that remains in the rock (*Nikolaeva et al., 2008*). Markers trace the amount of melt extracted during subduction. In the models, a constant  $M_{\text{max}} = 4 \text{ vol.}\%$  and  $M_{\text{max}}/M_{\text{min}} = 2$  ratio is used. The total amount of melt migrating upward is calculated as reported in *Nikolaeva et al. (2008)*. The extracted melt is instantaneously driven to the surface since the velocity of the melt is thought to be rapid compared to the deformation of the unmolten mantle and be unaffected from its dynamics (*Nikolaeva et al., 2008*).

### 3. Results

The systematic change of parameters in our models (serpentinite rheology, convergence rate, initial slab dip, age of the oceanic lithosphere, extent of pre-subduction serpentinitization, subduction zone – continental margins distance; initial weak-zone geometry) allowed us to assess the role of different processes governing the evolution

of an intraoceanic subduction zone, with particular regard to: i) the serpentinite channel geometry, ii) the subduction/exhumation dynamics and iii) the volcanic activity. Our models indicate that serpentinite rheology is a major factor controlling geometry and importantly the exhumation dynamics in the channel. In particular, the main features observed in models running a strong power-law rheology (wet olivine) and a weak Newtonian rheology will be compared with those of one model (model crdk; Table 2a) in which serpentinite is described by a weak power-law rheology (Hilaret et al., 2007). A final comparison is made among models with “heterogeneous” and layered oceanic crust.

### 3.1. Serpentinite channel geometry

In each model, water loss from subducting slab causes formation of a serpentinite layer at the plate/mantle interface. Serpentinite rheology strongly controls the geometry of the channel: a strong power-law behavior (wet olivine) enhances the formation of planar (Fig. 2A) or wedge channels (Fig. 2B), whereas a weak Newtonian creep of serpentinite induces planar or “hourglass” channels (Figs. 2D–3C). The last geometry evolves into a planar channel that develops a serpentinitic

bulge at the bottom (Fig. 3D). A weak power-law serpentinite rheology promotes development of wedge shapes evolving into planar channels during convergence process. Wedge channels are characterized by decreasing thickness with increasing depth, whereas thickness of planar channels is almost constant or slightly decreases towards high depths. “Hourglass” channels display maximum thickness at the bottom and at the top and are narrower at intermediate depths. Geometry of the channel is also extensively controlled by a number of major parameters such as the initial subduction dip angle, the age of the youngest oceanic lithosphere and the depth of the serpentinite horizon in the oceanic slab (Fig. 4). Convergence rate and the distance of subduction zone from the continental margins have a minor influence.

Hereafter we discuss the role of major critical parameters in dependence of rheological behavior of serpentinite.

#### 3.1.1. Initial slab dip

Subduction zones with low dip angle ( $15^\circ$ ) and serpentine strong power-law rheology (Fig. 2A) produce a channel with changing geometry: the channel is generally planar and assumes a wedge-like morphology at the beginning and during the final stages of subduction,

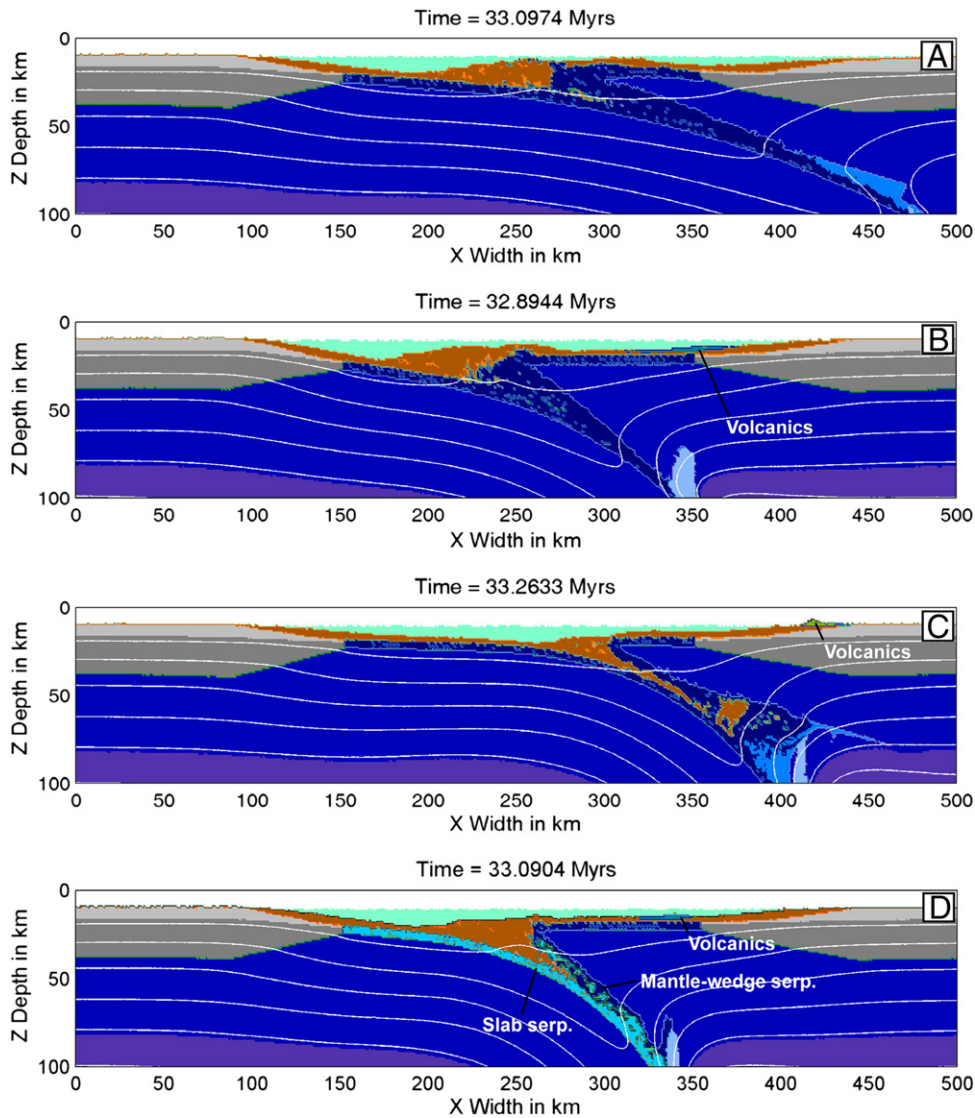


**Fig. 2.** Influence of slab dip considering two distinct serpentinite rheologies (A–B: strong power-law rheology (wet olivine); C–D: Newtonian rheology). a–c) shallow slab dip ( $15^\circ$ ; model crbo and crck); B–D) steep slab ( $40^\circ$ ; model crch and crco). The legend of colors is represented in Fig. 1. Explanation in the text.

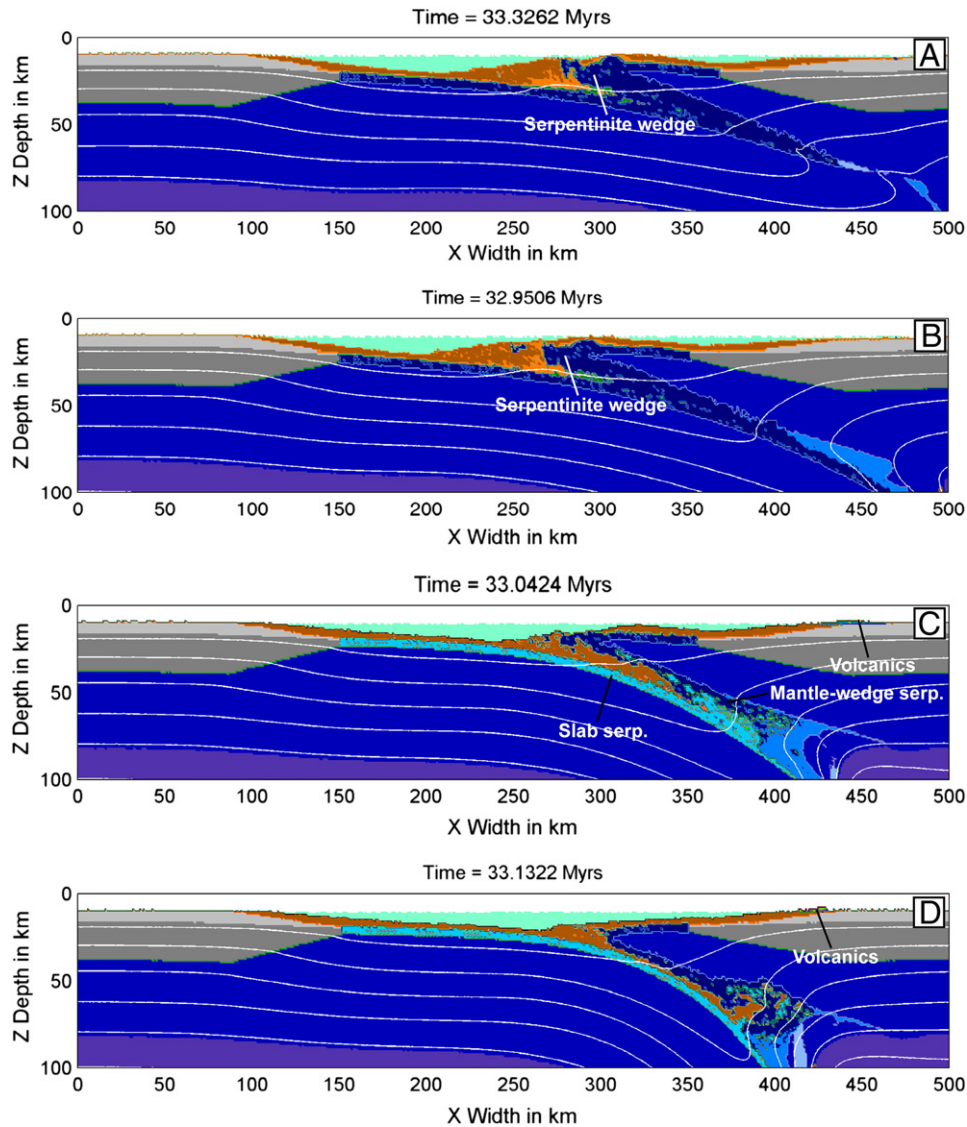


**Fig. 3.** Different serpentinite channel geometries obtained with variable ages of the youngest part of oceanic lithosphere. A–C) 5 My, development of a wedge shape channel (crbe) with a strong power-law (wet olivine) creep of serpentine and of an “hourglass” channel (crrc) considering a Newtonian creep of serpentine; B–D) 30 My, a planar channel (crbc) forms with a strong power-law serpentine rheology; a Newtonian behavior produces a serpentinite “bulge” at the bottom of the planar channel (crrc). In C) and D) the mixing between serpentinites scraped off the slab and those deriving from the hydration of mantle wedge is highlighted.

when the continental crust approaches to the trench. In such shallow subduction zones the main agent controlling the channel morphology is the migration of uprising slab-fluids: in the first stage of subduction the majority of serpentinites belong to the oceanic lithosphere and hydration affects a thin portion of the mantle wedge. With the subduction progress, fluids are released from an increasingly larger slab surface, conferring a planar shape to the channel. The approaching of the channel to the antigorite breakdown P–T conditions is responsible for its final wedge morphology. Steeper slabs ( $40^\circ$ ; strong power-law serpentine rheology) develop a well marked wedge-shape serpentinite channel during the whole convergence (Fig. 2B).

Using a Newtonian serpentine rheology, low angle-dipping slabs ( $15^\circ$ ) produce channels with an initial wedge shape that evolves first in a planar and then in an “hourglass” geometry. The pre-collisional stages are characterized by progressive formation of a serpentinite “bulge” that widens below the overriding plate (Fig. 2C). A narrow wedge-shaped channel develops in the initial stages of high-angle subduction ( $40^\circ$ ; Newtonian serpentine rheology); with the advancing process the channel acquires a broader and broader planar morphology (Fig. 2D).

### 3.1.2. Age of the oceanic lithosphere

At a given time after the subduction initiation, the P–T conditions of serpentinite breakdown are reached at shallower depths in young and hotter lithosphere (5 My) compared to older and colder slabs (30 My) (e.g. Fig. 3A–B). In models with strong power-law serpentine rheology, such conditions favor formation of shallow wedge-like channels in “hot” subduction zones (Fig. 3A); in contrast, stability of serpentinite to greater depths in older and colder oceanic plates allows development of planar channels (Fig. 3B). In case of Newtonian serpentine creep this situation is valid only for the initial stages of subduction; during the ongoing convergence both young and old slabs produce “hourglass” channels evolving to planar channels that broaden at increasing depths (Fig. 3C–D).

### 3.1.3. Extent of pre-subduction serpentinization

The initial depth of the serpentinization horizon in the oceanic lithosphere and hence the ratio between areas occupied by gabbro intrusions versus serpentinite also plays an important role. Greater serpentinite thickness (6 km), corresponding to a lithosphere where gabbros are 50% of serpentinites (two rows of  $2 \times 2$  km of gabbros;

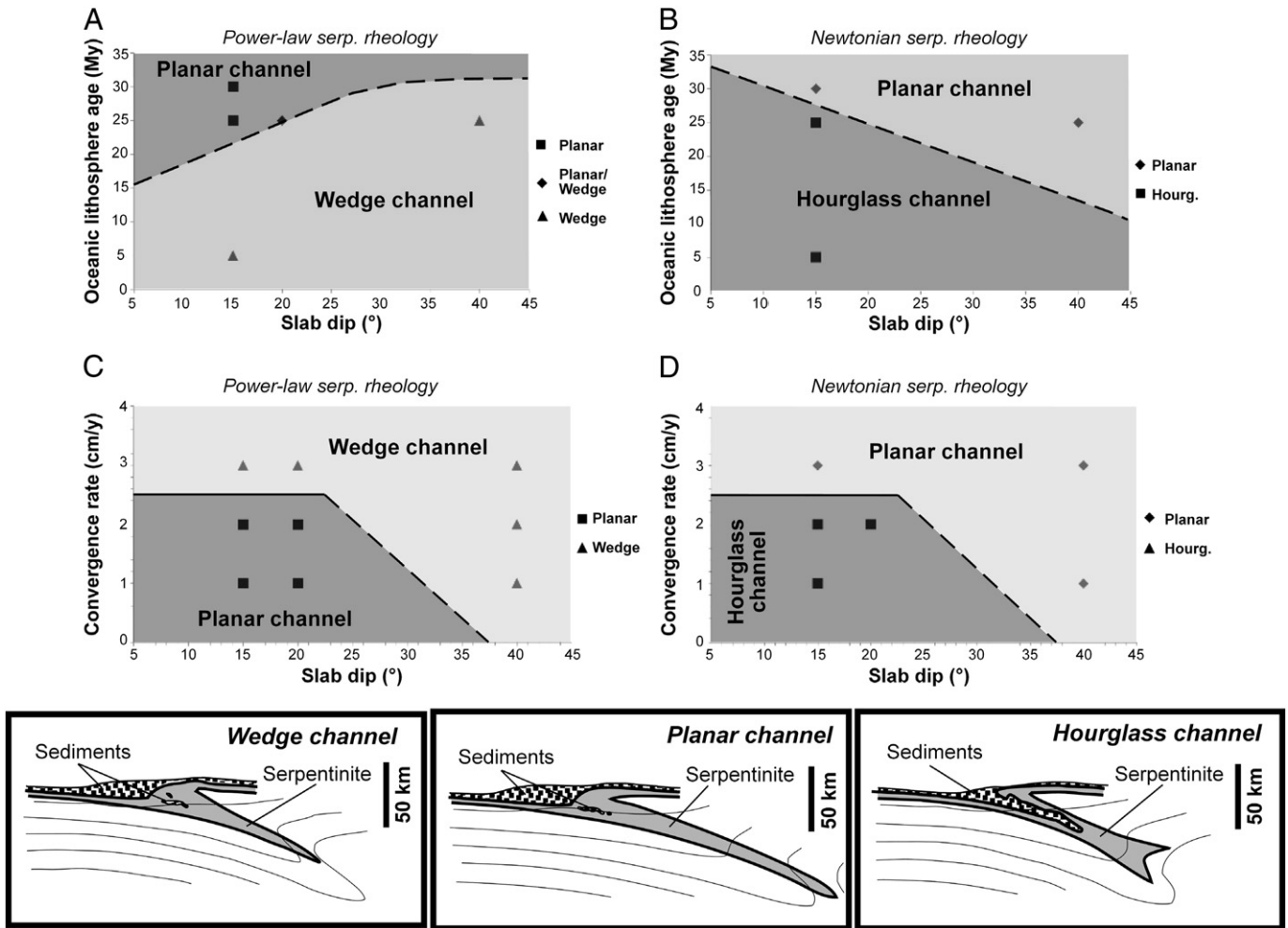


**Fig. 4.** Area diagrams showing the control on channel geometry of: A–B) age of the younger oceanic lithosphere vs slab dip; C–D) convergence rate vs slab dip (A–C: strong power-law serpentine rheology; b–d: Newtonian serpentine rheology). The symbols depict the observed results in models. The dashed lines are an inferred limit between two fields. The small cartoons represent the three end-members of the channel geometry.

Fig. 5A), induces development of wedge-shape channels. Less serpentinized lithosphere (2 km of serpentine thickness) with higher gabbro ratio (200%) leads to formation of planar channels (Fig. 5B).

Lighter and less dense oceanic lithosphere, e.g. where gabbros are 20% of the total serpentine (6 km of serpentinites and one row of 2×2 km gabbro pockets), is hardly subducted. This causes a strong

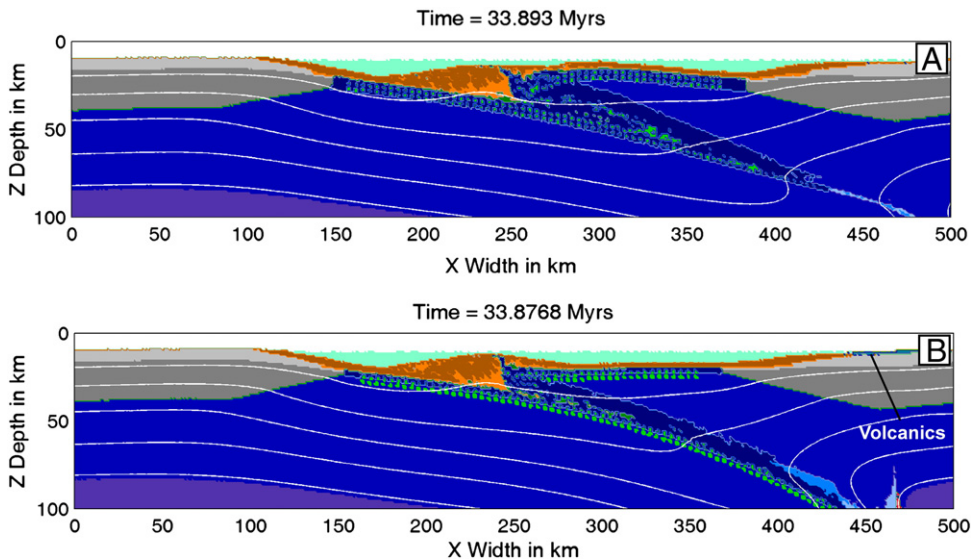


**Fig. 5.** Effect of slab structure. A) 6 km-thick serpentinite horizon in mantle peridotite (model craz); B) 2 km-thick serpentinite horizon (model crba).

decrease of the subduction rate; the continental crust is therefore unable to subduct and it starts to buckle. In this case gabbro intrusions reach maximum depths of about 40 km and no circulation is active inside the channel.

The serpentinization degree of the slab does not affect the channel geometry. An almost pure serpentinite (density = 2800 kg/m<sup>3</sup>) slows down the subduction process and inhibits the subduction of continental crust at depths > 40 km. To summarize, the higher is serpentinization of the subducting oceanic lithosphere, the less is the possibility of deep subduction.

### 3.1.4. Convergence rate

Velocity of the incoming plate does not considerably affect the channel geometry; in general high velocity values tend to produce wedge-shape instead of planar shape channels (serpentine strong power-law rheology) (Fig. 6A–B).

High convergence rate coupled with serpentinite Newtonian rheology slows down the velocity of hydration of the mantle wedge (Fig. 6C); this mechanism involves the development of a planar channel that only in the pre-collisional stages evolves in an hourglass geometry.

### 3.1.5. Distance of subduction zone from the continental margins

Distance of the weak zone from the continental margins usually has minor influence on the evolution of the channel, independently of serpentinite rheology. An exception is done for subduction with intermediate dip angles and convergence rate (20° and 2 cm/y) starting at an active continental margin (strong power-law rheology of serpentinite). The channel acquires a trapezium geometry that becomes more and more marked proceeding with the convergence; the asthenospheric mantle tends to rise along the subducting plate; due to the increase of temperature in the mantle wedge, the water release

and the formation of serpentine are restricted in a confined shallow area. A planar channel finally develops between the asthenospheric mantle and the subducting oceanic lithosphere.

## 3.2. Subduction and exhumation dynamics

Hereafter we will analyze the influence of major parameters (serpentinite rheology, initial slab dip, convergence rate, distance of the subduction zone from the continental margins) that control subduction and exhumation dynamics of oceanic lithosphere, sediments and mantle wedge rocks.

### 3.2.1. Serpentinite rheology

*Serpentinite rheology* is a key parameter for the dynamics inside the channel: a strong power-law serpentinite rheology inhibits mixing of oceanic serpentinite (here called “OS”) and crust with serpentinite deriving from hydration of the mantle wedge (MWS). In such a case a layered channel forms, with a top layer of MWS (delimited upward by the extent of the hydration front) and a lower layer of accreted oceanic slab materials. During subduction no mixing between OS and MWS occurs (Fig. 7A) independently of slab dip and velocity of the incoming plate.

On the other hand, the Newtonian serpentinite creep enhances the early mixing between OS (deriving both by the subducting slab and by the overriding plate) and MWS: variably sized blocks are torn from the slab and later incorporated and exhumed together with mantle-wedge serpentinites (Fig. 7B–C).

A weak power-law serpentinite rheology (Hilaret et al., 2007) produces a transitional behavior between those of strong power-law and weak Newtonian rheologies: inside the subduction channel greater mechanical mixing is observed compared to strong power-law models.

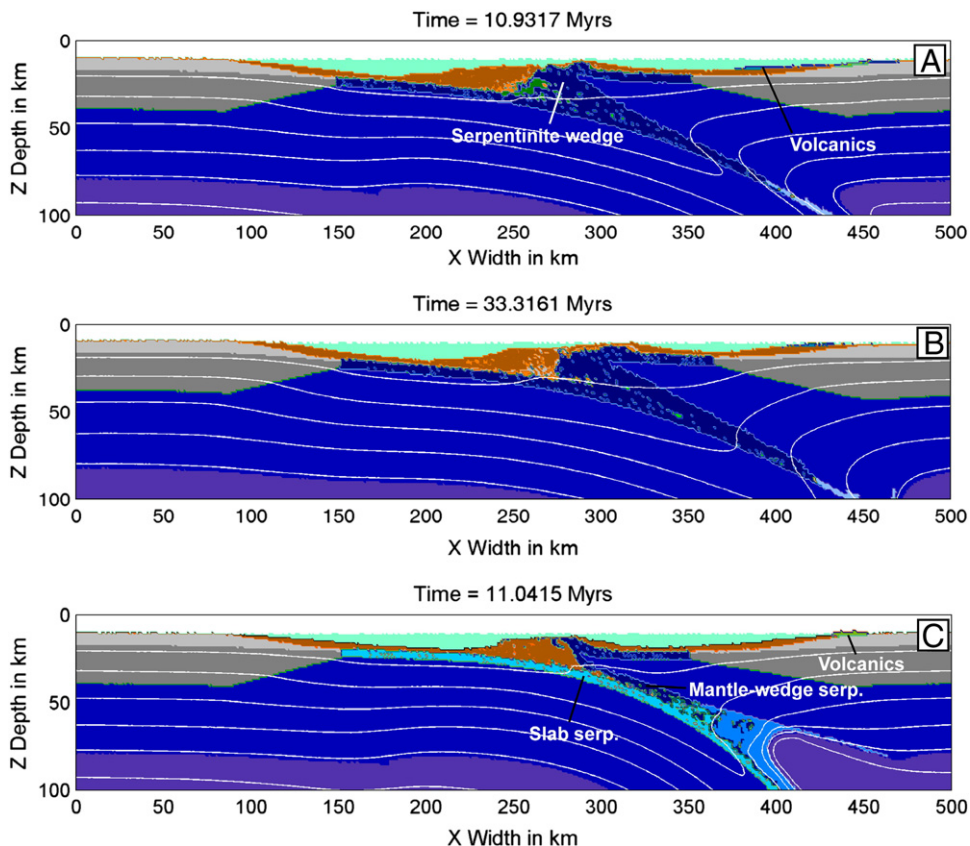


**Fig. 6.** Effect of convergence rate (A–B: strong power-law rheology of serpentinite; C and Fig. 2C: Newtonian rheology of serpentinite). A–C) high velocity (3 cm/y; model crbl and crcp); B and Fig. 2C) low velocity (1 cm/y; model crcb and crck in Fig. 2C).

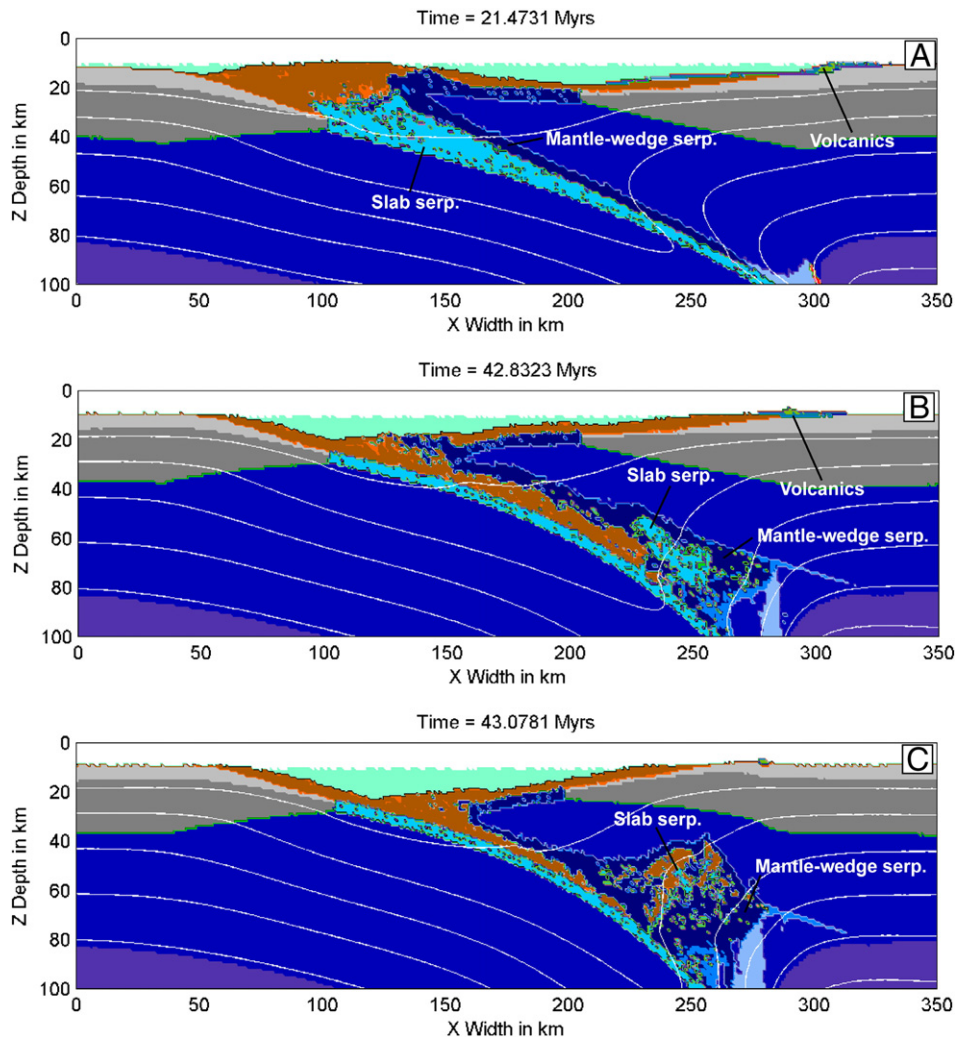


**Fig. 7.** Different mixing mechanisms inside the subduction channel; they are controlled by serpentine rheologies. A) strong power-law rheology (model *crci* = *crcb* with convergence rate = 2 cm/y); B) Newtonian rheology and young oceanic lithosphere (5 My; model *crcr*); C) Newtonian rheology and “old” oceanic lithosphere (30 My; model *crcs*).

### 3.2.2. Initial slab dip and convergence rate

Initial inclination of the slab and convergence rate are furthermore important parameters controlling the circulation of subducted rocks inside the serpentinite channel, especially in models adopting a Newtonian rheology of serpentinite. In this case serpentinite mixing starts at 400 °C isotherm depth considering shallow subduction zones (15°) and independently of convergence rate. 400 °C isotherm depth acts as a “barrier” for further subduction of the slices at the top of the slab, that are instead scraped off and accreted inside the serpentinitic “bulge”. During convergence, such a depth barrier varies and it increases according to the bending of isotherms. Buried rocks are exhumed from pressure greater than 20 kbar (see following paragraph). Steeply dipping subducting plates (40°) promote marked mixing of slab and wedge materials along the entire channel; the mixing effect decreases with increasing subduction velocity and exhumation is progressively inhibited.

Considering a strong power law serpentinite rheology, only blocks of lithosphere very close to the trench are partially exhumed (till 5 kbar) from maximum pressure of 10–15 kbar with an anticlockwise P–T path. High convergence rates (3 cm/y) promote a strong flux of slab bodies in the shallower part of the serpentinitic wedge (Fig. 6A) where they start to circulate making well defined loops. These rocks record initial anticlockwise P–T paths, followed by later clockwise paths reaching maximum pressure of about 5 kbar. Some of the involved rocks can be later dragged by the slab to higher depths but not be exhumed.

### 3.2.3. Distance of subduction zone from continental margins

The distance of the subduction zone from the continental margins affects the exhumation mechanism only in case of Newtonian creep of serpentinite: when the weak zone is located in the middle of the oceanic basin (250 km far from the “right” continental margin), the arrival of the continental crust at the trench is associated with a slight slab roll-back; during the collisional stages it triggers the exhumation of the buoyant serpentinitic mélangé along the channel (Fig. 8). Blocks of the downgoing oceanic lithosphere reach peak pressure >20 kbar and they record a broad clockwise exhumation path including an almost isothermal retrograde trajectory (Fig. 8). The overall P–T trajectory of the considered lenses includes minor burial-subduction cycles that anticipate the final exhumation stage.

If the subduction zone is closer to the continental margin, exhumation occurs with the vertical displacement of the buoyant serpentinitic mélangé, triggered by the asthenosphere upwelling, and it is instead inhibited along the slab. Portions of the serpentinitic mélangé can be accreted at the base of continental crust or they can stagnate under the overriding plate.

### 3.2.4. The fate of sediments

Sediments of both oceanic and continental origin are pushed by the subducting plate towards the trench and piled in an accretionary prism that progressively underthrusts the top of the serpentinite channel. If serpentinite deforms according to a strong power-law, only a small

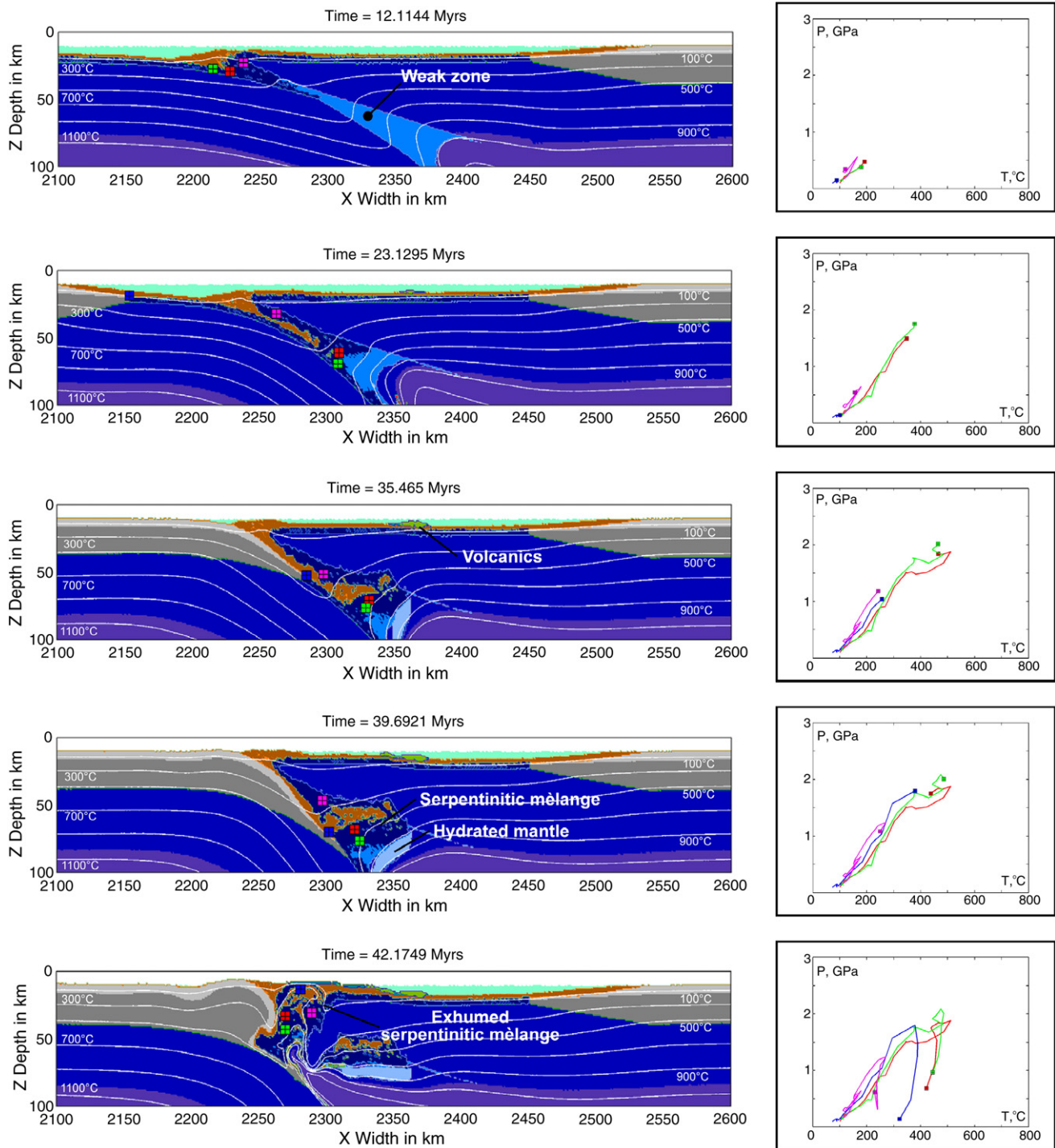


**Fig. 8.** Subduction and exhumation of two metagabbro lenses (red and green squares), a metasediment block (blue square) and serpentinite body (pink square). On the left their paths in 2D dimensions are represented; the boxes on the right depict their trajectories in the P–T space. The model has the same characteristics of model crck, except for the distance of the subduction zone from the right continental margin (250 km).

amount of sediments ( $\sim 10\text{--}20\text{ km}^2$ ) is usually subducted before collision: the majority of sediments is pushed to depth by the downgoing continental crust but is never exhumed. Low-angle slab dip and young oceanic lithosphere favor mixing between sediments and serpentinite: oceanic sediments form kilometer-size isolated bodies inside the channel that reach shallow depth and are not exhumed. Sediments belonging to the areas closest to the continental margins are first accreted at the base of the accretionary prism and later exhumed inside it, following a clockwise P–T trajectory. A similar behavior occurs considering a weak power-law serpentinite rheology (Hilaret et al., 2007).

The Newtonian creep of serpentinite allows transport towards high pressures of a greater amount of sediments dragged by the downgoing slab. The blocks have kilometer- to pluri-kilometer-size; they reach the “barrier” depth defined by the 400 °C isotherm and are mixed together with serpentinite. Such behavior is valid only for shallow slabs; in steeper or fast subduction settings only a small amount of sediments can reach high depths. Fast slabs produce a bigger and well developed accretionary prism compared to slow subduction (Fig. 6C). Moreover considering young slabs, subduction of sediments starts about 10 My later compared to old slabs.

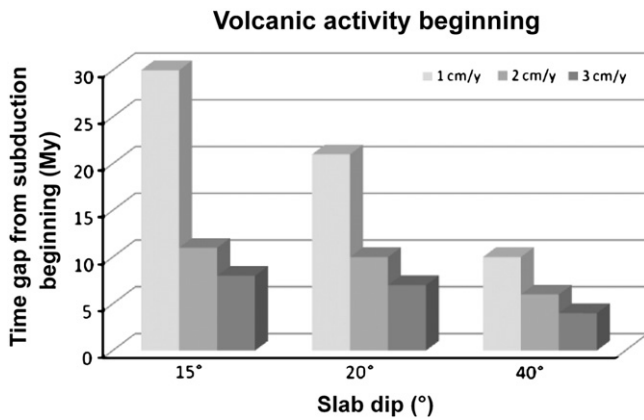


Fig. 9. Volcanic activity age (after beginning of subduction) as function of convergence rate and slab dip (strong power-law rheology of serpentinite).

During progressive convergence the accretionary sedimentary prism can incorporate blocks of the top of the serpentinite wedge; in case of strong power-law serpentinite rheology this behavior is shown only by relatively old oceanic lithosphere.

### 3.3. Volcanic activity

The volcanic activity related to melt migration from mantle depths is strongly controlled by the geometry of the slab, the convergence rate and the age of the oceanic lithosphere considering either a strong power-law or a Newtonian serpentinite rheology. In particular, steep and fast slabs are characterized by earlier eruption of volcanic products (Fig. 9); furthermore if the slab inclination is high, the volcanic front is closer to the trench and the volcanic activity is more widespread and abundant compared to shallow and slow subduction (Fig. 10). The arc-trench gap is always > 110–120 km as reported by Marshak and Karig (1977, and references therein) for present-day systems (Table 2a–b). In models with Newtonian serpentinite rheology the linear extension of volcanics is generally minor compared to models with a strong power-law serpentinite rheology.

In our models volcanic fronts are usually localized on continental crust, since most models count for an intraoceanic subduction zone close to the continental margin. Subduction zones far from the continental margin are characterized by formation of volcanic fronts inside the oceanic basin.

The volcanic products mainly derive from melting of mantle peridotite and gabbro; a minor amount is related to melting of subducted continental crust and basalts. Great part of the produced melt is

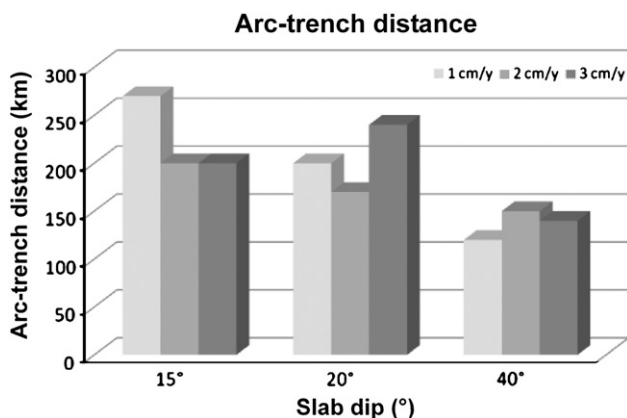


Fig. 10. The diagram depicts the distance between volcanics spreading area and trench as function of convergence rate and slab dip (strong power-law rheology of serpentinite).

probably due to the input in the deep mantle of water released from the complete subduction of OS and MWS.

The volcanic activity is also controlled by the age of the oceanic lithosphere since the melting process is triggered a few million years earlier in young slabs compared to older ones. In the first case the volcanic front is also closer to the trench and its extension at a fixed time is minor.

The subduction of dense oceanic lithosphere (with 2 km of abyssal serpentinite, model crba) induces an early and widespread upward migration of melts; the structure of oceanic lithosphere does not affect the arc-trench distance.

### 3.4. Alternative weak-zone geometries

The beginning of subduction at a trapezium-shape shallow weak-zone at the base of the serpentinitized mantle peridotites (as described in Section 2) is preceded by formation of a kilometric scale open fold in the shallow part of the oceanic lithosphere. The direction of subduction is a function of the friction coefficient of the weak zone. Low values (0.1) imply a “rightward” dipping slab (Fig. 11A–B; Table 2; craq model); a wide serpentinitic prism with a funnel morphology forms and gabbro and basalts reach maximum depths of about 50 km inside it. Sediments are partly accumulated in the trench and in the frontal part of the serpentinitic wedge but they do not contribute to form an accretionary prism. The first magmatic activity appears about 38 My after the beginning of subduction, 160 km far from the trench. After 40 My, the volcanic arc is only 10 km wide (Table 2a). Greater friction coefficients of the weak zone (0.2–0.3) produce the passive downward bending of the oceanic lithosphere close to the continental right-margin and the beginning of a “left-ward” dipping subduction. The volcanic activity begins 28 My later on the “left-side” plate and after 40 My it is extended about 30 km. A shallow weak zone that reaches the continental right margin and a weak zone with high-friction coefficient involve subduction processes with similar characteristics.

Experiments with a uniform age of the oceanic lithosphere results in a vertical serpentinitic prism with a flower-like structure (Fig. 11C–D; base model: craq); the subduction is symmetric, double-sided and gabbros and basalts stagnate at shallow depths. Sediments subduct only in the final stages before continental crust obduction. In the same setting, higher values of the friction coefficient (0.2–0.3) involve exhumation of the subducted continental crust in the serpentinitic prism till superficial depths and an active circulation in the shallower parts of the serpentinitic prism. Volcanic activity is absent.

### 3.5. Comparison with a “layered” oceanic crust

We compared subduction of oceanic lithosphere with “heterogeneous” structure with that of layered oceanic lithosphere. In the latter case the crust is made of a continuous gabbro layer 3.5 km-thick, overlain by a 2.5 km-thick basalt layer. At the top a 500 m-thick sedimentary cover is present. Convergence rate is 1 cm/y and the initial slab dip is 15° (Table 2a–b).

#### 3.5.1. Strong power-law serpentinite rheology (wet olivine)

A serpentinite layer develops between the subducting plate and the mantle wedge; it is almost parallel to the slab and it inhibits the effective exhumation of subducted slab blocks as the correspondent models with a non-layered lithosphere (model crbo). Compared to a “heterogeneous” lithosphere, the layered lithosphere models show a younger volcanic activity with larger extension on the surface and comparable distances from the trench.

#### 3.5.2. Weak Newtonian serpentinite rheology (constant viscosity of $10^{18}$ Pa s)

These models show that a planar serpentinite channel forms above the subducting slab; the thickness of the channel is greater in

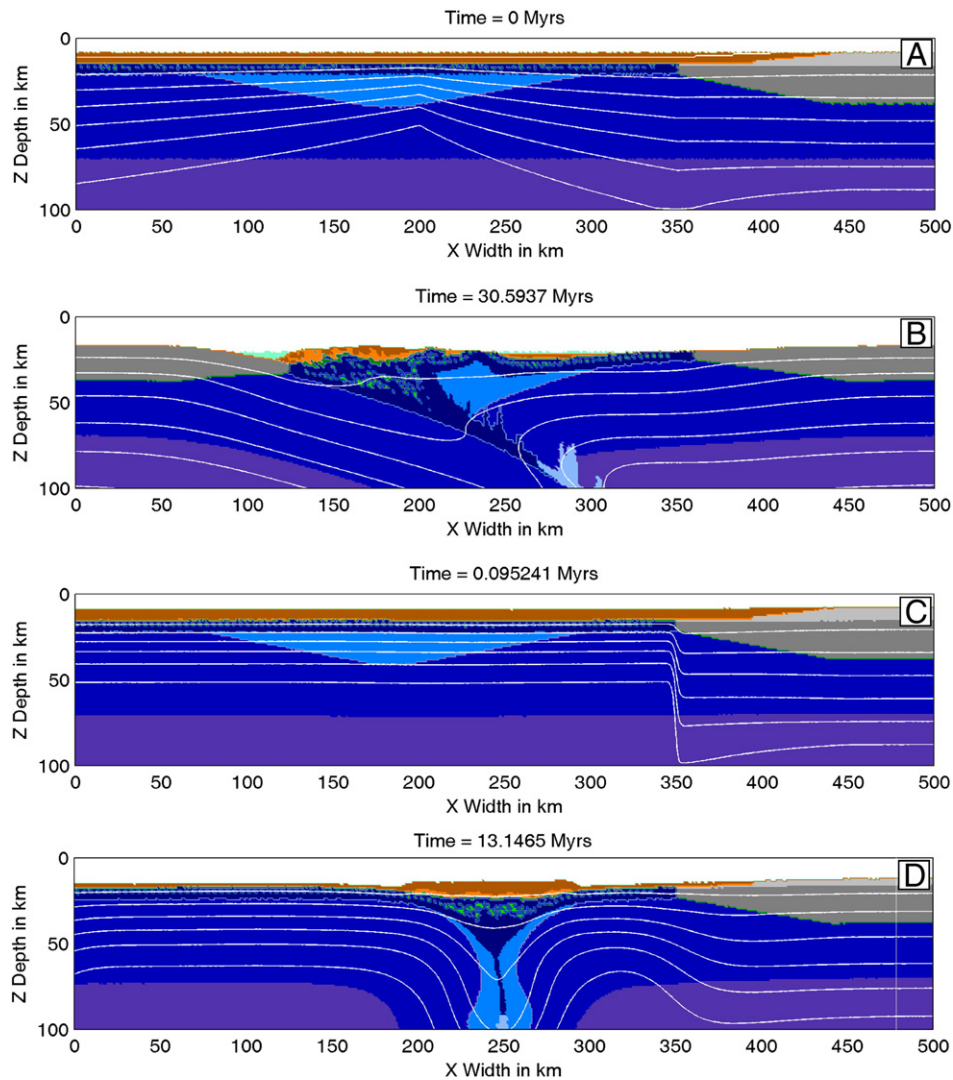


**Fig. 11.** Trapezium-shape weak zone. The age of the oceanic lithosphere influences the style of subduction. A–B) the oceanic lithosphere becomes younger towards the inner parts of the basin (10 My) and a rightward subduction starts; C–D) a homogeneous age of the oceanic lithosphere (10 My) produces a double-side subduction.

the first 40 km and decreases deeper. Sediments are only partially buried inside the channel and reach shallow depth (about 30 km). The great part of slab slices is exhumed from depth of about 50–60 km inside mantle wedge serpentinites that completely wrap them. Exhumation is related to coupled slab retreat and asthenospheric mantle upwelling along the subducting plate. Differently from the reference case with “heterogeneous” lithosphere (model crk), exhumation is contemporaneous to subduction of the oceanic plate, the serpentinite channel is wider and develops a slightly different geometry; moreover a minor amount of sediments is subducted. Compared to the reference case, the volcanic activity develops on a wider surface of the continental margin and derives from melting of the subducted oceanic gabbro and in minor part of basalt. Moreover, decompression melting of the asthenospheric mantle induces the extension of the fore-arc oceanic crust and the formation of new oceanic floor in a supra-subduction environment.

#### 4. Discussion

The numerical models presented here clarify the main processes allied with intra-oceanic subduction within a narrow, slow-spreading basin. Past in the Earth history closure of comparably small basins has played a key role in formation of orogens like the Alps: in some branches of these immature oceans the oceanic

lithosphere was subducted below a thinned continental crust, in other branches, like for instance the Piemontese-Ligurian Tethys, subduction was intraoceanic. Our study thus better applies to the latter settings, whose evolution gave rise to vast exposures of high-pressure metamorphic ophiolites. All models presented here show that dehydration fluids arising from the subducting oceanic plate determine widespread mantle serpentinization in the overriding plate to form a channel where accretion and upward flow of slab materials are established. This serpentinite channel is the major feature of all models. Its shape is controlled by initial dip angle of subduction, age of incoming oceanic lithosphere and extent of pre-subduction serpentinization. The dynamics of the channel vary with initial slab dip, convergence rate and distance of subduction from the continental margins. Serpentinite rheology controls both the geometry and exhumation dynamics. Moreover, tests on different weak zone geometries suggest that an effective subduction process occurs only if the weak zone is a down-dipping plane that initially drives the subducting slab into depth.

##### 4.1. Effects of different rheology and deformation mechanisms

Due to the extreme abundance of antigorite serpentinite in the slab and in the overlying mantle, serpentinite rheology has revealed to be the most important physical parameter that affects geometry of the

channel and the whole architecture of the plate interface. We observed three main geometries of the channel: planar, wedge-like and “hourglass”. As shown in Fig. 4, strong power-law serpentine rheology (wet olivine) promotes development of planar and wedge channels; differently, weak Newtonian serpentine deformation involves formation of planar and “hourglass” channels.

In case of strong power-law rheology, the main structure of the plate interface is layered and shows a subducting serpentinized plate and a serpentinized mantle wedge layer that are separated from each other. Slices of slab are in fact continuously accreted at the base of mantle-wedge. Very limited mixing thus occurs in the channel between elements of the subducting plate and overlying mantle. Considering strong power-law creep, steep slabs or high convergence rate, a wedge-type geometry of the channel prevails; planar channels are associated with low velocities or shallow slabs. Old slabs or minor thickness of the serpentinized horizon in the oceanic lithosphere, considering a constant proportion of gabbro pockets, produce planar channels. We have observed that in models adopting strong power-law rheology, sediments are not involved in deep subduction: at least during the early evolutionary stages, they do not mix in the channel and stay at shallow levels in the subduction system. Only with late-stage collision and subduction of the continental plate, they become subducted to slightly deeper levels. In practice, adopting this rheological behavior, sediment subduction and mixing of sedimentary slices into the channel is not very effective.

The models running a weak Newtonian serpentine creep show the formation of serpentinitic channels in which the rocks offscraped from the slab and its sedimentary cover are subducted and stored at great depths. In the deep levels of the subduction zone a serpentinite bulge forms as the result of accumulation of a tectonic *mélange* made of slab materials mixed with hydrated mantle wedge (Fig. 8). The geometry of the channel however varies during time from initial wedge shape to planar and hourglass in the intermediate stages; a final funnel shape characterizes the pre-collisional stages during which the channel is almost completely closed at the top under the sedimentary accretionary prism. In the last stages the channel has reduced thickness at shallow depths and progressively widens to increasing depth where the mixing mechanism develops.

The two serpentine rheologies also determine different burial and exhumation behaviors inside the channel:

- shallow circulation inside the serpentinite wedge, enhanced by high convergence rate, prevails using a strong power-law rheology. Bodies scraped off the oceanic slab and its sedimentary cover are mixed in the superficial serpentinitic wedge and are exhumed even after few cycles of burial;
- the Newtonian deformation of serpentinite involves stronger mixing of the oceanic slab with sediments inside the serpentinitic channel. An important feature emerging from models adopting Newtonian behavior concerns the mode of exhumation of the deep *mélange* zone forming the bulge shown in Fig. 8. This *mélange* is exhumed at the onset of collision and in the late stages of continental subduction; the combination of slight slab roll-back, collision of the continental crust and presence of weak serpentinized mantle allows upwelling of the asthenospheric mantle. Such mechanism, linked with the density contrast between the channel and the surrounding mantle triggers the exhumation of the serpentinitic *mélange*. Several authors (Agard et al., 2009; Chemenda et al., 1995; Gorczyk et al., 2007; Guillot et al., 2009; Platt, 1993; Schwartz et al., 2001) have discussed the efficient role of buoyancy for the exhumation of high- and ultrahigh-pressure rocks. Moreover Hermann et al. (2000) pointed out that serpentinite is a good carrier for the exhumation of dense eclogite since the low-density of serpentine lowers the bulk density of the high-pressure terrain below mantle values. Sediments are

exhumed in the channel together with slab slices and serpentinites deriving from the hydration of mantle wedge.

The comparison of models adopting different serpentinite rheology suggests that dynamics within the serpentinite channel is best described by a weak Newtonian rheology. Differently from strong power law-controlled serpentinite, Newtonian creep enhances deep burial and exhumation of slab slices and sediments, as observed in several HP metaophiolitic massifs worldwide. Importantly, this type of rheology enables deep burial of sediments, as observed in high-pressure terrains, and points to buoyancy-driven exhumation, roughly concomitant with continental subduction and slab roll-back.

Our results partly contrast with those of Hilaiet and Reynard (2009), who studied a 1-D model serpentinized channel. Hilaiet and Reynard (2009) obtained an active exhumation assuming that serpentine rheology was described by a relatively weak power-law creep (Hilaiet et al., 2007). Same as our models running either strong or weak power-law rheology, Hilaiet and Reynard (2009) predicted a narrowing of the channel with increasing depths; the channel is in fact 8–10 km-thick at shallow levels and reaches maximum thickness of 2–3 km at great depths. Hilaiet and Reynard (2009) propose that exhumation from great depths (more than ~60 km) is driven by serpentinite acting as low density carrier; at intermediate depths (between 15 and 50 km) upward flow of HP rocks is caused by the pressure gradient linked with narrowing of the channel. This behavior is not observed in our simulations running either strong or weak power-law rheology. Hilaiet and Reynard (2009) however considered that exhumation of HP rocks in the interval 15–50 km can happen even if a vast low density serpentinized region is located at high depths, as happens in our models running a Newtonian serpentinite rheology; in our models the channel has in fact a minimum thickness at intermediate depths and widens at increasing pressure developing a “bulge” at its bottom. Indeed we should mention that our models with weak power law rheology of serpentine show to some degree transitional behavior between the strong power-law and weak Newtonian models: more mechanical mixing is observed inside the subduction channel and sediments become subducted to moderate depths during transition from subduction to collision.

The rheology of serpentinite does not affect noticeably the volcanic activity even if a Newtonian creep of serpentine is responsible for a minor superficial extension of the volcanic layer. Steep and fast slab are characterized by an early production of volcanics; the spreading center is generally closer to the trench in steep subduction. Young oceanic lithosphere produces a younger volcanic activity located close to the trench compared to old slabs as proposed by Cross and Pilger (1982).

#### 4.2. Provenance of high-pressure rocks within the channel

Our models running Newtonian serpentinite creep highlight that materials of different provenance are tectonically sliced in the channel. Besides oceanic lithosphere and oceanic sediments, the subduction channel *mélange* also contains continental sediments and slices of serpentinized mantle from the upper plate. This is shown in Fig. 8, tracing the physical pathways within the model of particles belonging to the above mentioned settings. Importantly, sediments of continental affinity are pushed to depth by the subducting continental crust, are accreted to the subduction *mélange* and are exhumed to the surface. The age of oceanic lithosphere can influence the size of both sedimentary and slab-derived bodies inside the mantle wedge serpentinites: a young oceanic lithosphere allows the presence of kilometer-size coherent bodies (Fig. 6B) whereas old slabs promote mingling of sediments and slab bodies (Fig. 6C). Fig. 8 also emphasizes that two types of high-pressure serpentinite (deriving from the altered slab mantle or from the hydrated mantle wedge) become closely associated and are mixed with sediments of different origin

within the channel. Slab bodies are in fact closely associated and wrapped by mantle wedge serpentinite.

This observation seems to be partially validated by natural evidence. Serpentinities exposed in HP-LT terrains are in fact usually attributed to two geological environments: mantle wedge (e.g. Himalayan serpentinites) (Guillot et al., 2001, 2004; Hattori and Guillot, 2007) or lithospheric serpentinites of the oceanic slab (e.g. Alpine serpentinites) (Guillot et al., 2004; Scambelluri et al., 1995). Both types of serpentinite were however observed in Northern Dominican Republic, Eastern and Central Cuba (Blanco-Quintero et al., 2011b; Hattori and Guillot, 2007; Saumur et al., 2007, 2010). Saumur et al. (2010) however propose that mantle wedge serpentinite occurs along late major strike-slip fault zones and the serpentinite hosting the tectonic mélanges could derive from abyssal serpentinites. Hattori and Guillot (2007) and Lewis et al. (2006) suggested a prevalence of hydrothermalized serpentinites.

#### 4.3. Comparison with Alpine high-pressure ophiolites

The rock slices (Fig. 8) that in our model are tectonically mixed in the subduction zone display different provenance, pressure-temperature metamorphic paths and are expected to couple at different times in the mélangé. These features could be taken as guidelines to assess a correspondence of processes depicted in the models with processes that likely operated in nature during emplacement of high-pressure terrains in Alpine-type orogens. The South-Western Alps derive from a former intraoceanic subduction system (Hoogerduijn Strating, 1991; Malavieille et al., 1998; Marroni and Pandolfi, 2007 and references therein; Marroni and Treves, 1998; Molli and Tribuzio, 2004; Schwartz et al., 2007; Van Wamel, 1987) and include several HP-LT ophiolitic massifs like Voltri and Monviso. Other high- and ultrahigh-pressure ophiolite like Zermatt-Saas correspond to oceanic lithosphere subducted below a continental plate. The above massifs may disclose some evolutionary features fitting with the model evolutions we propose here.

In particular, our models better fit with the Voltri high-pressure ophiolites. The Voltri Massif (south-eastern sector of the Western Alps) comprises different tectono-metamorphic units recording variable P-T peak metamorphic conditions ranging from the blueschist to

the eclogitic facies. Highly sheared serpentinite and subordinate metasediments of both oceanic and continental origin wrap bodies of metagabbro and metabasite which are tens of meters to hundred meter-sized (Capponi and Crispini, 2002; Cortesogno et al., 1975; Federico et al., 2005 and references therein; Malatesta et al., 2011). A serpentinitic mélangé including metric to decametric lenses of metagabbro, metabasite and metasediment was recognized within the large coherent units of Voltri Massif by Federico et al. (2007a). These authors related its exhumation to the contribution of a serpentinite subduction channel. Malatesta et al. (2011) propose that the same mechanism acted at kilometer-scale exhuming at least the eastern sector of the Voltri Massif. Several mafic and ultramafic bodies of this ophiolitic massif record scattered peak P-T conditions and similar exhumation trajectories (Fig. 12A). Our model (Fig. 8) highlights that gabbro and serpentinite bodies included in the serpentinite channel record different peak P-T values. These values are comparable to those recorded by the Voltri high-pressure rocks; in particular, a good agreement exists with high-pressure metamorphic peaks; the low pressure metamorphic peaks in the model show lower temperature compared to the natural case. Moreover, both the simulated and natural P-T paths are clockwise, thus recording higher temperature during exhumation compared to burial, suggesting that a steady state thermal structure was already achieved in the subduction zone (Gerya et al., 2002). The exhumation trajectories are almost isothermal and slightly cooling (Figs. 8 and 12a); according to what is depicted in the model, the lack of a strong cooling of Voltri Massif rocks during decompression could be related to the fact that exhumation is coeval with relaxation of isotherms occurred during the stop of subduction. The channel incorporated both oceanic and continental sediments (e.g. blue square, Fig. 8) that, as in the Voltri Massif, are wrapped by serpentinite. These features suggest that the exhumation of the Voltri Massif was driven by coupling/decoupling mechanisms acting inside a low viscosity buoyant serpentinite channel.

The case of the HP-LT Monviso Massif (South-Western Alps) is debated. According to some authors (Groppo and Castelli, 2010; Guillot et al., 2004, 2009; Lombardo et al., 1978; Schwartz et al., 2000) it is composed of several metaophiolitic tectono-metamorphic units recording different P-T paths; in this massif eclogite lenses of several km long are surrounded by serpentinite. Several authors

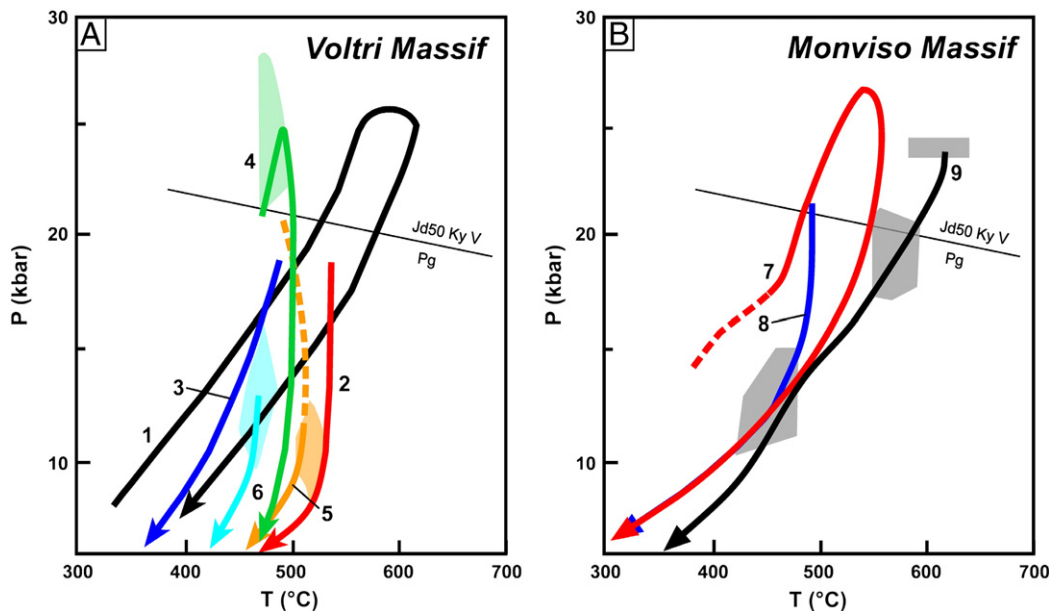


**Fig. 12.** Representative P-T paths of Voltri (A) and Monviso (B) massifs. (A) – 1 = Scambelluri et al., 1995; 2 = Federico et al., 2004; 3 = Liou et al., 1998; 4,5,6 = Malatesta et al., 2011. Colored areas show different peak conditions for the Voltri Massif after Malatesta et al., 2011. (B) – 7 = Angiboust et al., 2011 – partially derived from Groppo and Castelli, 2010 and Schwartz et al., 2000; 8 = Angiboust et al., 2011; 9 = Schwartz et al., 2000, Agard et al., 2010. Gray areas depict different peak conditions of Monviso Massif after Schwartz et al., 2000.

attribute its exhumation to the presence of a serpentinized subduction channel (Guillot et al., 2004; Schwartz et al., 2001, 2007). These authors report various P–T peaks shown in Fig. 12B: this points to variable burial depths reached by the various slices composing the Monviso “mélange”, that can be grouped together is a subduction channel following the models proposed here. A different interpretation has been recently proposed by Angiboust et al. (2011), who propose that the Monviso ophiolites can be grouped in two coherent tectonic subunits (Monviso and Lago Superiore units) with a peak pressure gap of about 3–4 kbar; as a consequence, the Lago Superiore Unit should not be considered as a chaotic serpentinite mélange. According to Angiboust et al. (2011), these units were detached from the slab at different depths and later juxtaposed at epidote–blueschist facies conditions during exhumation along the subduction interface. In both cases either relatively small slices, or larger coherent slabs of subducted oceanic materials can be accreted and tectonically coupled in domains at the plate interface where mantle atop of the slab is serpentinized and softened, so to enhance detachment and tectonic coupling of slab materials. In the case of Monviso interpretations, what importantly changes is the size of bodies involved in the channel. P–T paths can be considered as a first evidence of the possible exhumation of the Monviso Massif through a serpentinite matrix as shown in our model: the Monviso P–T trajectories (Fig. 12B) show in fact, similarly to the model and to the Voltri Massif, clockwise path and slightly cooling retrograde paths with almost comparable high-pressure peaks.

The general validity of the exhumation process proposed for the two above mentioned natural cases is besides testified by the following evidences:

- P–T gradient represented in Fig. 8 follows a general cool subduction trend (about 8 °C/km) comparable to that highlighted by Agard et al. (2009) for the case of Western Alps;
- the P–T path traced by a serpentinite body in the model (pink square, Fig. 8) contains a “hair-pin” type segment; this peculiar trajectory retraces the burial path at low T and it thus indicates a first cold exhumation stage active during subduction (Blanco-Quintero et al., 2011a; Krebs et al., 2008). According to what is predicted by the model, multiple burial–exhumation cycles have been highlighted in the Western Alps by Beltrando et al. (2007) and Rubatto et al. (2011);
- the main exhumation stage in the model occurs during subduction of the continental crust and the beginning of collision as suggested for the Western Alps by Agard et al. (2009);
- the exhumation velocities of metagabbro lenses and serpentinite inside the channel are in the range of mm/y; these values fit the estimates proposed by Agard et al. (2009) for worldwide oceanic rocks and in particular for those of the Monviso and Voltri massifs (Agard et al., 2009; Federico et al., 2005; Hoogerduijn Strating, 1991; Vignaroli et al., 2010).

Moreover, the model shows that slices of the overriding oceanic plate are progressively eroded and dragged into deep mantle inside the serpentinite channel (pink square, Fig. 8) (ablative subduction) and stored inside the serpentinite mélange. This particular feature, together with previous simulations by Faccenda et al. (2009), Roda et al. (2010), Stöckhert and Gerya (2005), Tao and O’Connell (1992) supports the theory of several authors (e.g. Clift and Vannucchi, 2004; Platt, 1986) who proposed that, besides the slab, slices of the overriding plate are torn away and buried together with the subducting slab. Polino et al. (1990) and Spalla et al. (1996) applied this concept to the Austroalpine domain (Western Alps) which includes slices of the Adria overriding continental margin. Finally, Tonarini and Scambelluri (2010), based on isotopic rock compositions, suggested that a portion of Voltri Massif serpentinite could possibly represent a slice of the overriding oceanic mantle.

## 5. Conclusions

Numerical models presented here show that intraoceanic subduction within a narrow slow-spreading oceanic basin produces a low-viscosity serpentinite channel characterized by different geometries and internal dynamics. The geometry of the channel is controlled by major parameters as slab dip, age and structure of the subducting oceanic lithosphere. The variation in slab dip, convergence rate and distance of subduction from the continental margins drives on the other hand different subduction and exhumation dynamics inside the channel. Serpentinite rheology is however the key parameter controlling both the geometry and exhumation mechanisms. Our simulations show that a weak Newtonian serpentinite creep best describes subduction and exhumation mechanisms of oceanic lithosphere, sediments and mantle-wedge serpentinite that mix together at high-pressure conditions. During convergence slices of the overriding oceanic plate can be scraped off and dragged till great depth into the channel. In particular, our models highlight that abyssal and mantle-wedge serpentinites can be incorporated together in the channel. The serpentinite mélange is exhumed from great depth after subduction of the continental crust and at onset of collision and buoyancy is the driving force. Continental crust thus plays an important role in stopping subduction and triggering exhumation of high-pressure rocks. We moreover propose that the formation of a serpentinite channel, acting as a low-viscosity carrier for high density subducted rocks, could be considered responsible for the exhumation of Alpine ophiolitic massifs as the HP Voltri and Monviso massifs.

Finally, our numerical experiments suggest that the subduction of even very narrow inter-continental oceanic basins may lead to development of a magmatic arc. We found that for such relatively small and short-lived arcs, steeper, faster and younger slabs produce earlier onset of volcanism after subduction initiation.

## Acknowledgments

We thank two anonymous reviewers for the detailed constructive revisions. This study was financially supported by PRIN-COFIN 2007 to Marco Scambelluri, by PRIN-COFIN 2008 to Giovanni Capponi, and by the University of Genova. Taras Gerya acknowledges support by ETH Research Grants ETH-0807-2, ETH-0807-3, ETH-0609-2, SNF Research Grants 200020-126832, 200020-129487, Crystal2Plate program, SNF ProDoc program 4-D-Adamello and TopoEurope Program.

## Appendix A. Supplementary data

Supplementary data to this article can be found online at doi:10.1016/j.lithos.2012.01.003.

## References

- Abbate, E., Bortolotti, V., Principi, G., 1980. Apennines ophiolites: a peculiar oceanic crust, in: Rocci, G. (Eds), Tethyan ophiolites, Western area. *Ophioliti Special Issue* 1, 59–96.
- Agard, P., Yamato, P., Jolivet, L., Burov, E., 2009. Exhumation of oceanic blueschists and eclogites in subduction zones: timing and mechanisms. *Earth-Science Reviews* 92, 53–79.
- Angiboust, S., Langdon, R., Agard, P., Waters, D., Chopin, C., 2011. Eclogitization of the Monviso ophiolite (Western Alps) and implications on subduction dynamics. *Journal of Metamorphic Geology*. doi:10.1111/j.1525-1314.2011.00951.x.
- Arcay, D., Tric, E., Doin, M.P., 2005. Numerical simulations of subduction zones. Effect of slab dehydration on the mantle wedge dynamics. *Physics of the Earth and Planetary Interiors* 149, 133–153.
- Beltrando, M., Hermann, J., Lister, G., Compagnoni, R., 2007. On the evolution of orogens: pressure cycles and deformation mode switches. *Earth and Planetary Science Letters* 256, 372–388.
- Bittner, D., Schmeling, H., 1995. Numerical modeling of melting processes and induced diapirism in the lower crust. *Geophysical Journal International* 123, 59–70.
- Blanco-Quintero, I.F., García-Casco, A., Gerya, T.V., 2011a. Tectonic blocks in serpentinite mélange (eastern Cuba) reveal large-scale convective flow of the subduction channel. *Geology* 39, 79–82.

- Blanco-Quintero, I.F., Proenza, J.A., García-Casco, A., Tauler, E., Galí, S., 2011b. Serpentinized and serpentinites within a fossil subduction channel: La Corea mélange, eastern Cuba. *Geologica Acta* 9, 389–405.
- Boccaletti, M., Elter, P., Guazzone, G., 1971. Plate tectonic models for the development of the western Alps and northern Apennines. *Nature* 234, 108–111.
- Bostock, M.G., Hyndman, R.D., Rondenay, S., Peacock, S.M., 2002. An inverted continental Moho and serpentinization of the forearc mantle. *Nature* 417, 536–538.
- Burov, E.B., Jolivet, L., Le Pourhiet, L., Poliakov, A., 2001. A thermomechanical model of exhumation of HP and UHP metamorphic rocks in Alpine mountain belts. *Tectonophysics* 342, 113–136.
- Capponi, G., Crispini, L., 2002. Structural and metamorphic signature of Alpine tectonics in the Voltri Massif (Ligurian Alps, North-Western Italy). *Eclogae Geologicae Helvetiae* 95, 31–42.
- Chemenda, A.I., Mattauer, M., Malavieille, J., Bokun, A.N., 1995. A mechanism for syn-collisional rock exhumation and associated normal faulting: results from physical modelling. *Earth and Planetary Science Letters* 132, 225–232.
- Clauser, C., Huenges, E., 1995. Thermal conductivity of rocks and minerals. In: Ahrens, T.J. (Ed.), *Rock Physics and Phase Relations: AGU Reference Shelf*, 3, pp. 105–126.
- Clift, P., Vannucchi, P., 2004. Controls on tectonic accretion versus erosion in subduction zones: implications for the origin and recycling of the continental crust. *Review of Geophysics* 42 (RG2001), 1–31.
- Cloos, M., 1982. Flow mélanges: numerical modeling and geologic constraints on their origin in the Franciscan subduction complex, California. *Geological Society of America Bulletin* 93, 330–345.
- Cortesogno, L., Galli, M., Messiga, B., Pedemonte, G.M., Piccardo, G.B., 1975. Nota preliminare alla petrografia delle rocce eclogitiche del Gruppo di Voltri (Liguria Occidentale). *Res Ligusticae CLXXXIX*, Estratto dagli Annali del Museo Civico di Storia Naturale di Genova, LXXX.
- Cross, T.A., Pilger Jr., R.H., 1982. Controls of subduction geometry, location of magmatic arcs, and tectonics of arc and back-arc regions. *Geological Society of America Bulletin* 93, 545–562.
- Dick, H.J.B., Lin, J., Schouten, H., 2003. An ultraslow-spreading class of ocean ridge. *Nature* 426, 405–412.
- Dick, H.J.B., Natland, J.H., Ildefonse, B., 2006. Past and future impact of deep drilling in the oceanic crust and mantle. *Oceanography* 19, 72–80.
- Dilek, Y., Moores, E.M., Delaloye, M., Karson, J.A., 1991. Amagmatic extension and tectonic denudation in the Kizildag ophiolite, southern Turkey: implication for the evolution of Neotethyan oceanic crust. In: Peters, T.J., et al. (Ed.), *Ophiolite genesis and evolution of the oceanic lithosphere*, pp. 485–500.
- Duret, T., May, D.A., Gerya, T.V., Tackley, P.J., 2011. Discretization errors and free surface stabilization in the finite difference and marker-in-cell method for applied geodynamics: a numerical study. *Geochemistry, Geophysics, Geosystems* 12, Q07004.
- Escartin, J., Hirth, G., Evans, B., 2001. Strength of slightly serpentinized peridotites: implications for the tectonics of oceanic lithosphere. *Geology* 29 (11), 1023–1026.
- Faccenda, M., Minelli, G., Gerya, T., 2009. Coupled and decoupled regimes of continental collision: numerical modeling. *Earth and Planetary Science Letters* 278, 337–349.
- Federico, L., Capponi, G., Crispini, L., Scambelluri, M., 2004. Exhumation of alpine high pressure rocks: insights from petrology of eclogite clasts in the Tertiary Piedmontese basin (Ligurian Alps, Italy). *Lithos* 74, 21–40.
- Federico, L., Capponi, G., Crispini, L., Scambelluri, M., Villa, I.M., 2005. <sup>39</sup>Ar/<sup>40</sup>Ar dating of high-pressure rocks from the Ligurian Alps: evidence for a continuous subduction–exhumation cycle. *Earth and Planetary Science Letters* 240, 668–680.
- Federico, L., Crispini, L., Scambelluri, M., Capponi, G., 2007. Different PT paths recorded in a tectonic mélange (Voltri Massif, NW Italy): implications for the exhumation of HP rocks. *Geodinamica Acta* 20, 3–19.
- García-Casco, A., Torres-Roldán, R.L., Iturralde-Vinent, M.A., Millán, G., Núñez Cambra, K., Lázaro, C., Rodríguez Vega, A., 2006. High pressure metamorphism of ophiolites in Cuba. *Geologica Acta* 4, 63–88.
- Gerya, T., Stöckhert, B., 2006. Two-dimensional numerical modeling of tectonic and metamorphic histories at active continental margins. *International Journal of Earth Science (Geologische Rundschau)* 95, 250–274.
- Gerya, T.V., Yuen, D.A., 2003. Characteristics-based marker-in-cell method with conservative finite-differences schemes for modeling geological flows with strongly variable transport properties. *Physics of the Earth and Planetary Interiors* 140, 295–320.
- Gerya, T.V., Yuen, D.A., 2007. Robust characteristics method for modelling multiphase visco-elasto-plastic thermo-mechanical problems. *Physics of the Earth and Planetary Interiors* 163, 83–105.
- Gerya, T.V., Stöckhert, B., Perchuk, A.L., 2002. Exhumation of high-pressure metamorphic rocks in a subduction channel: a numerical simulation. *Tectonics* 21 (6), 1–15 1056.
- Gorczyk, W., Guillot, S., Gerya, T.V., Hattori, K., 2007. Asthenospheric upwelling, oceanic slab retreat, and exhumation of UHP mantle rocks: insights from Greater Antilles. *Geophysical Research Letters* 34 (L21309), 1–5.
- Groppo, C., Castelli, D., 2010. Prograde P–T Evolution of a lawsonite eclogite from the monviso meta-ophiolite (Western Alps): dehydration and redox reactions during subduction of oceanic FeTi-oxide gabbro. *Journal of Petrology* 51, 2489–2514.
- Guillot, S., Hattori, K.H., de Sigoyer, J., Nägler, T., Auzende, A.L., 2001. Evidence of hydration of the mantle wedge and its role in the exhumation of eclogites. *Earth and Planetary Science Letters* 193, 115–127.
- Guillot, S., Schwartz, S., Hattori, K., Auzende, A., Lardeaux, J.M., 2004. The Monviso ophiolitic Massif (Western Alps), a section through a serpentinite subduction channel. In: Beltrando, M., Lister, G., Ganne, J., Boullier, A. (Eds.), *Evolution of the Western Alps: insights from metamorphism, structural geology, tectonics and geochronology: Journal of the Virtual Explorer*, 16. Paper 3.
- Guillot, S., Hattori, K., Agard, P., Schwartz, S., Vidal, O., 2009. Exhumation processes in oceanic and continental subduction contexts: a review. In: Lallemand, S., Funiello, F. (Eds.), *Subduction Zone Geodynamics*. Springer-Verlag, Berlin Heidelberg, pp. 175–205.
- Hattori, K.H., Guillot, S., 2007. Geochemical character of serpentinites associated with high-to ultrahigh-pressure metamorphic rocks in the Alps, Cuba, and the Himalayas: recycling of elements in subduction zones. *Geochemistry, Geophysics, Geosystems* 8 (Q09010) 27 pp.
- Hermann, J., Müntener, O., Scambelluri, M., 2000. The importance of serpentinite mylonites for subduction and exhumation of oceanic crust. *Tectonophysics* 327, 225–238.
- Hilaret, N., Reynard, B., 2009. Stability and dynamics of serpentine layer in subduction zone. *Tectonophysics* 465, 24–29.
- Hilaret, N., Reynard, B., Wang, Y., Daniel, I., Merkel, S., Nishiyama, N., Petitgirard, S., 2007. High-pressure creep of serpentine, interseismic deformation and initiation of subduction. *Science* 318, 1910–1913.
- Hirose, T., Bystricky, M., Kunze, K., Stünitz, H., 2006. Semi-brittle flow during dehydration of lizardite–chrysotile serpentinite deformed in torsion: implications for the rheology of oceanic lithosphere. *Earth and Planetary Science Letters* 249, 484–493.
- Hoogerduijn Strating, E.H., 1991. The evolution of the Piemonte–Ligurian ocean. A structural study of ophiolite complexes in Liguria (NW Italy). PhD thesis. University of Utrecht, 127 pp.
- Hyndman, R.D., Peacock, S.M., 2003. Serpentinization of the forearc mantle. *Earth and Planetary Science Letters* 212, 417–432.
- Ildefonse, B., Blackman, D.K., John, B.E., Ohara, Y., Miller, D.J., MacLeod, C.J., Integrated Ocean Drilling Program Expeditions 304/305 Science Party, 2007. Oceanic core complexes and crustal accretion at slow-spreading ridges. *Geology* 35, 623–626.
- Katayama, I., Hiraochi, K.I., Michibayashi, K., Ando, J.I., 2009. Trench-parallel anisotropy produced by serpentine deformation in the hydrated mantle wedge. *Nature* 461, 1114–1117.
- Krebs, M., Maresch, W.V., Schertl, H.P., Munker, C., Baumann, A., Draper, G., Idlemann, B., Trapp, E., 2008. The dynamics of intra-oceanic subduction zones: a direct comparison between fossil petrological evidence (Rio San Juan Complex, Dominican Republic) and numerical simulation. *Lithos* 103, 106–137.
- Krebs, M., Schertl, H.P., Maresch, W.V., Draper, G., 2011. Mass flow in serpentinite-hosted subduction channels: P–T–t path patterns of metamorphic blocks in the Rio San Juan mélange (Dominican Republic). *Journal of Asian Earth Sciences* 42, 569–595.
- Lagabriele, Y., Cannat, M., 1990. Alpine jurassic ophiolites resemble the modern central Atlantic basement. *Geology* 18, 319–322.
- Lagabriele, Y., Lemoine, M., 1997. Alpine, Corsican and Apennine ophiolites: the slow-spreading ridge model. *Earth and Planetary Science Letters* 150, 909–920.
- Leat, P.T., Larter, R.D., 2003. Intra-oceanic subduction systems: introduction. *Geological Society, London, Special Publications* 219, 1–17.
- Lewis, J.F., Draper, G., Proenza, J.A., Espaillet, J., Jiménez, J., 2006. Ophiolite-related ultramafic rocks (serpentinites) in the Caribbean region: a review of their occurrence, composition, origin, emplacement and Ni-laterite soil formation. *Geologica Acta* 4, 237–263.
- Liou, J.G., Zhang, R., Ernst, W.G., Liu, J., McLimans, R., 1998. Mineral parageneses in the Piampaludo eclogitic body, Gruppo di Voltri, Western Ligurian Alps. *Schweizer Mineralogische und Petrographische Mitteilungen* 78, 317–335.
- Lombardo, B., Nervo, R., Compagnoni, R., Messiga, B., Kienast, J.R., Mevel, C., Fiora, L., Piccardo, G.B., Lanza, R., 1978. Osservazioni preliminari sulle ofioliti metamorfiche del Monviso (Alpi Occidentali). *Rendiconti della Società Italiana di Mineralogia e Petrologia* 34, 253–305.
- Malatesta, C., Crispini, L., Federico, L., Capponi, G., Scambelluri, M., 2011. The exhumation of high pressure ophiolites (Voltri Massif, Western Alps): insights from structural and petrologic data on metagabbro bodies. *Tectonophysics*. doi:10.1016/j.tecto.2011.08.024.
- Malavieille, J., Chemenda, A., Larroque, C., 1998. Evolutionary model for Alpine Corsica: mechanism for ophiolite emplacement and exhumation of high-pressure rocks. *Terra Nova* 10, 317–322.
- Marroni, M., Pandolfi, L., 2007. The architecture of an incipient oceanic basin: a tentative reconstruction of the Jurassic Liguria–Piemonte basin along the Northern Apennines–Alpine Corsica transect. *International Journal of Earth Sciences (Geologische Rundschau)* 96, 1059–1078.
- Marroni, M., Treves, B., 1998. Hidden terranes in the Northern Apennines, Italy: a record of late Cretaceous–Oligocene transpressional tectonics. *Journal of Geology* 106, 142–162.
- Marroni, M., Meneghini, F., Pandolfi, L., 2010. Anatomy of the Ligure–Piedmontese subduction system: evidence from Late Cretaceous–middle Eocene convergent margin deposits in the Northern Apennines, Italy. *International Geology Review* 52, 1160–1192.
- Marshak, R.S., Karig, D.E., 1977. Triple junctions as a cause for anomalously near-trench igneous activity between the trench and volcanic arc. *Geology* 5, 233–236.
- McQuarrie, N., Stock, J.M., Verdel, C., Wernicke, B.P., 2003. Cenozoic evolution of Neotethys and implications for the causes of plate motions. *Geophysical Research Letters* 30 (2036), 1–4.
- Meda, M., Marotta, A., Spalla, M., 2010. The role of mantle hydration into the continental crust recycling in the wedge region. *Geological Society, London, Special Publications* 332, 149–172.
- Mevel, C., 2003. Serpentinization of abyssal peridotites at mid-ocean ridges. *Comptes Rendus Geoscience* 335, 825–852.
- Molli, G., Tribuzio, R., 2004. Shear zones and metamorphic signature of subducted continental crust as tracers of the evolution of the Corsica/Northern Apennine orogenic system. In: Alsop, G.I., Holdsworth, R.E., McCaffrey, K.J.W., Handy, M. (Eds.), *Flow processes in faults and shear zones: Geological Society, London, Special Publications*, 224, pp. 321–335.
- Nikolaeva, K., Gerya, T.V., Connolly, J.A.D., 2008. Numerical modelling of crustal growth in intra-oceanic volcanic arcs. *Physics of the Earth and Planetary Interiors* 171, 336–356.

- Piccardo, G.B., 2007. Evolution of the ultra-slow spreading Jurassic Ligurian tethys: view from the mantle. *Periodico di Mineralogia* 76, 67–80 Special Issue 1: from Petrogenesis to Orogenesis.
- Platt, J.P., 1986. Dynamic of orogenic wedges and the uplift of high-pressure metamorphic rocks. *Geological Society of America Bulletin* 97, 1037–1053.
- Platt, J.P., 1993. Exhumation of high pressure rocks: a review of concepts and processes. *Terranova* 5, 119–133.
- Poli, S., Schmidt, M.W., 1995. H<sub>2</sub>O transport and release in subduction zones: experimental constraints on basaltic and andesitic system. *Journal of Geophysical Research* 100 (B11), 22299–22314.
- Polino, R., Dal Piaz, G.V., Gosso, G., 1990. Tectonic erosion at the Adria margin and accretionary processes for the Cretaceous orogeny of the Alps. *Società Geologica Italiana* 1, 345–367.
- Ranalli, G., 1995. *Rheology of the Earth*. Chapman and Hall, London. 413 pp.
- Roda, M., Marotta, A.M., Spalla, M.I., 2010. Numerical simulations of an ocean-continent convergent system: influence of subduction geometry and mantle wedge hydration on crustal recycling. *Geochemistry, Geophysics, Geosystems* 11, 1–21.
- Rubatto, D., Regis, D., Hermann, J., Boston, K., Engi, M., Beltrando, M., McAlpine, S.R.B., 2011. Yo-yo subduction recorded by accessory minerals in the Italian Western Alps. *Nature Geoscience* 4, 338–342.
- Saumur, B.M., Hattori, K.H., Guillot, S., 2007. Protrusion of fore-arc mantle serpentinites together with HP and UHP rocks along major strike-slip faults in the northern subduction complex of Dominican Republic. Paper presented at Subduction Zone Geodynamics Conference, Geoscience Montpellier Research Group, Montpellier, France, 4–7 June.
- Saumur, B.M., Hattori, K.H., Guillot, S., 2010. Contrasting origins of serpentinites in a subduction complex, northern Dominican Republic. *Bulletin of the Geological Society of America* 122, 292–304.
- Scambelluri, M., Müntener, O., Hermann, J., Piccardo, G.B., Trommsdorff, V., 1995. Subduction of water into the mantle: history of an Alpine peridotite. *Geology* 23, 459–462.
- Schmeling, H., Babeyko, A.Y., Enns, A., Faccenna, C., Funicello, F., Gerya, T., Golabek, G.J., Grigull, S., Kaus, B.J.P., Morra, G., Schmalholz, S.M., van Hunen, J., 2008. A benchmark comparison of spontaneous subduction models — towards a free surface. *Physics of the Earth and Planetary Interiors* 171, 198–223.
- Schmidt, M.W., Poli, S., 1998. Experimentally based water budgets for dehydrating slabs and consequences for arc magma generation. *Earth and Planetary Science Letters* 163, 361–379.
- Schwartz, S., Lardeaux, J.M., Guillot, S., Tricart, P., 2000. Diversité du métamorphisme écolitique dans le massif ophiolitique du Monviso (Alpes Occidentales, Italie). *Geodinamica Acta* 13, 169–188.
- Schwartz, S., Allemand, P., Guillot, S., 2001. Numerical model of the effect of serpentinites on the exhumation of eclogitic rocks: insights from the Monviso ophiolitic massif (Western Alps). *Tectonophysics* 42, 193–206.
- Schwartz, S., Lardeaux, J.M., Tricart, P., Guillot, S., Labrin, E., 2007. Diachronous exhumation of subducted HP metamorphic rocks from southwestern Alps: evidences from fission track analysis. *Terranova* 19, 133–140.
- Sizova, E., Gerya, T., Brown, M., Perchuk, L.L., 2010. Subduction styles in the Precambrian: insight from numerical experiments. *Lithos* 116, 209–229.
- Spalla, M., Lardeaux, J., Dal Piaz, G., Gosso, G., Messiga, B., 1996. Tectonic significance of Alpine eclogites. *Journal of Geodynamics* 21, 257–285.
- Stöckhert, B., Gerya, T.V., 2005. Pre-collisional high pressure metamorphism and nappe tectonics at active continental margins: a numerical simulation. *Terranova* 17, 102–110.
- Tao, W.C., O'Connell, R.J., 1992. Ablative subduction: a two-sided alternative to the conventional subduction model. *Journal of Geophysical Research* 97 (B6), 8877–8904.
- Takahashi, M., Uehara, S.I., Mimzoguchi, K., Masuda, K., 2011. On the transient response of serpentine (antigorite) gouge to stepwise changes in slip velocity under high-temperature conditions. *Journal of Geophysical Research* 116 25 pp.
- Tonari, S., Scambelluri, M., 2010. Boron and Strontium isotope systematics in deeply subducted alpine-serpentinites: evidence of high-11B fluid flow. EGU General Assembly 2010, Vienna, p. 4451.
- Turcotte, D.L., Schubert, G., 2002. *Geodynamics*. Cambridge University Press, p. 456.
- Ulmer, P., Trommsdorff, V., 1995. Serpentine stability to mantle depths and subduction-related magmatism. *Science* 268, 858–861.
- Van Wamel, W.A., 1987. On the tectonics of the Ligurian Apennines (Northern Italy). *Tectonophysics* 142, 87–98.
- Vignaroli, G., Rossetti, F., Rubatto, D., Theye, T., Lisker, F., Phillips, D., 2010. Pressure-temperature-deformation-time (P-T-d-t) exhumation history of the Voltri Massif HP complex, Ligurian Alps, Italy. *Tectonics* 29 (TC6009), 1–35.
- Warren, C.J., Beaumont, C., Jamieson, R.A., 2008. Modelling tectonic styles and ultrahigh pressure (UHP) rock exhumation during the transition from oceanic subduction to continental collision. *Earth and Planet Science Letters* 267, 129–145.
- Yamato, P., Agard, P., Burov, E., Le Pourhiet, L., Jolivet, L., Tiberi, C., 2007. Burial and exhumation in a subduction wedge: mutual constraints from thermo-mechanical modeling and natural P–T–t data (Sch. Lustrés, W. Alps). *Journal of Geophysical Research* 112 (B07410), 1–28.
- Yamato, P., Burov, E., Agard, P., Le Pourhiet, L., Jolivet, L., 2008. HP–UHP exhumation during slow continental subduction: self-consistent thermodynamically and thermomechanically coupled model with application to the Western Alps. *Earth and Planet Science Letters* 271, 63–74.
- Yamato, P., Husson, L., Braun, J., Loiselet, C., Thieulot, C., 2009. Influence of surrounding plates on 3D subduction dynamics. *Geophysical Research Letters* 36 (L07303), 1–5.